Journal of Plant Growth Regulation (2022) 41:1726–1746
https://doi.org/10.1007/s00344-021-10413-3

Application of Iron Oxide Nanoparticles as Micronutrient Fertilizer in Mulberry Propagation

Md Salman Haydar[1] · Suravi Ghosh[1] · Palash Mandal[1]

Received: 13 June 2020 / Accepted: 3 June 2021 / Published online: 20 June 2021

Abstract
Nanomaterials are practically used in every aspects of modern life, agriculture is one of them. The aim of this study was to evaluate the bio-effectiveness of iron oxide and EDTA functionalized iron oxide nanoparticles as a nano-micronutrient fertilizer to replace traditional Fe-fertilizer. The responses of these fertilizers were evaluated on growth and development of mulberry (*Morus alba* L.) plants in a pot experiment. Iron oxide nanoparticles and its EDTA functionalized form had been applied in two different dosage (10 and 50 mg/kg soil) by both soil application and foliar spray. Applications of these green synthesized nanoparticles showed an increased influence on morpho-physiochemical attributes in treated plants. Iron oxide nanoparticles application at a rate of 10 mg/kg in soil significantly improved morphological traits like sprouting percentage, number of leaves (52.73% improved over control), plant biomass (37.20% and 90.24% increase of shoot and root biomass over control, respectively), root attributes (34% increment for root length) and also shortened the first leaf appearance period. The same treatment showed an improvement of 42% and 15% over control in case of chlorophyll and sugar content, respectively. Efficacy of antioxidant enzymes like CAT, POD and NOX were also found to be enhanced over control. Together, these results showed that our treated nanoparticles could replace traditional Fe-fertilizer in the cultivation and propagation of mulberry crop. To the best of our knowledge, this is the first report on the effect of iron oxide nanoparticles and EDTA functionalized iron oxide nanoparticles as a nano-micronutrient fertilizer on mulberry growth and yield.

Handling Editor: Durgesh Kumar Tripathi.

✉ Palash Mandal
pmandalbotppprl@nbu.ac.in

[1] Nanobiology and Phytotherapy Laboratory, Department of Botany, University of North Bengal, Siliguri, West Bengal 734013, India

Graphic Abstract

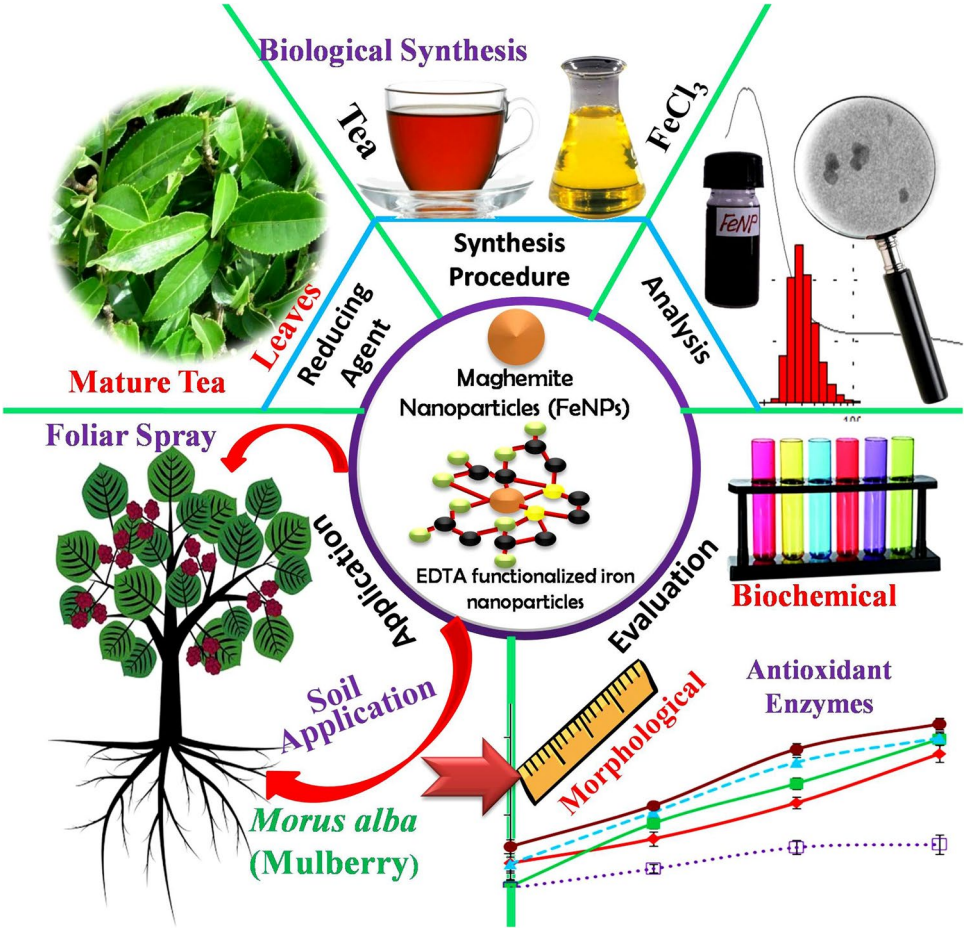

Keywords Iron oxide nanoparticles · EDTA-functionalized iron oxide nanoparticles · Nano-fertilizer · Mulberry · Plant growth

Introduction

Mulberry is a high biomass producing, fast-growing, perennial, woody plant belonging to the genus *Morus* under the family Moraceae (Pan and Lou 2008; Yang et al. 2010). Mulberry leaves, especially those of the *Morus alba* L. (white mulberry) is agriculturally more important, serving as sole food for monophagous insect *Bombyx mori* (silkworm larvae), the product of which (raw silk) puts impact on economy of a country like India. It is estimated that almost 90% of global raw silk production depends upon mulberry silk and in India mulberry silk culture was performed mainly by moriculture (mulberry plant culture). According to Food and Agriculture Organization of the United Nations (FAO), sericulture provides gainful employment, helping significantly to the livelihood of many people across the globe, plays an important role in anti-poverty program especially in the rural areas. Propagation of Mulberry depends upon vegetative method, seed germination, grafting and rarely by tissue culture. Propagation through stem cutting is the most simplest and cost effective vegetative proliferation practice used for mass production. However, this propagation method shows major delay in appearance of first leaf and sometimes in root succession, which ultimately delaying the harvesting time. Succession and rooting of cuttings greatly depends upon several factors like time of preparation of cuttings, cultivar chosen to obtain cuttings, physiological condition of the cuttings, environmental condition, application of hormones, fertilizers and nutritional supplement etc. (Hartmann et al. 2002). As suggested previously by various researchers for appropriate root establishment, growth and leaf production, a proper nutrient management system is required (Lu et al. 2003). Though micronutrients like iron, copper, zinc, manganese are required in very low amount, but presence of

correct balance of these elements is essential for growth and quality leaf production as they play vital role in development of plants (Hänsch and Mendel 2009; Noor-Ul-Din 2012). As stated by Geetha et al. (2017), in case of multi micronutrient deficiency in Mulberry, yield can be reduced even up to fifty percent. Among all these, to date, iron deficiency and its remediation were found to be the biggest agronomic challenges (Tagliavini et al. 2000; Li and Lan 2017). Though in the earth's crust, iron is the fourth most abundant element but a large proportion of this remain in the insoluble Fe^{+3} form, but as plants usually absorb iron in Fe^{+2} form from the soil, deficiency occur (Kobayashi and Nishizawa 2012; Mimmo et al. 2014; Bindraban et al. 2015; Ye et al. 2015). Its availability is also highly restricted to the plants grown in neutral to basic pH of aerobic soil (Straub et al. 2001). Due to low solubility of oxidized ferric form in aerobic atmosphere, iron is the third most limiting nutrient for growth and metabolism of a plant (Zuo and Zhang 2011; Samaranayake et al. 2012). However, iron is an indispensable nutrient for all organisms as it is the key determinant of various cellular metabolism such as electron transport system, biosynthesis of chlorophyll and cytochrome, respiration (Kim and Rees 1992), nutrient uptake, nitrogen fixation, DNA and protein synthesis (Rout and Sahoo 2015). Deficiency of iron is frequent in mulberry, growing in alkaline soils and exhibits symptoms of chlorosis. To address the deficiency, application of chemical and chelated iron fertilizers is adopted. Chelated fertilizers are quite costly and often applied for high value crops. Besides this, over or improper application of fertilizers under aerobic condition can generate reactive oxygen species (ROS) as by-products of Fenton reaction that may damage vital cellular components of plants (Rout and Sahoo 2015). Use of chemical fertilizer is an age long practice leads to soil mineral imbalance, destroy soil fertility, soil texture and shows long term effect to the ecosystem (Elemike et al. 2019). Biofertilizers to some extend play potential roles in improvement of soil fertility and crop production (Bhardwaj et al. 2014) but large-scale productions of biofertilizers are not easy and in some cases, they are pH and temperature dependent.

To deal with all the associated problems, incorporation of nanotechnology in agriculture arises which serves as the latest technology for precision agriculture. Nanomaterials consist of nano-scale particles having a diameter of less than 100 nm (Auffan et al. 2009). Because of their unique properties, novel features such as inherent biocompatibility, super-paramagnetism, enhanced surface to volume ratio, nanoparticles have been extensively used in many aspects of daily life of which agriculture holds an important position (Rastogi et al. 2017). Several earlier reports suggested the ability of nanoparticles in seed germination encouragement, degradation of pesticide residue and improvement of soil quality (Ghrair et al. 2010; El-Temsah et al. 2014). Our current study deals with the hypothesis that both soil and foliar application of iron oxide nanoparticles and EDTA functionalized iron oxide nanoparticles on mulberry propagation will improve the overall growth parameters.

Our study mainly emphasizes on enhancing the spouting percentage, decreasing the duration of leaf appearance and improving the overall vigour of Mulberry by application of phyto-synthesized iron oxide nanoparticles (FeNP) and EDTA functionalized iron oxide nanoparticles (FeNP EDTA).

Materials and Methods

Collection of Plant Materials

Mature, diseases free Tea [*Camellia sinensis* (L.) Kuntze] leaves for biosynthesis of iron oxide nanoparticles were collected from Tea garden, University of North Bengal, Siliguri, West Bengal, India (26°42′41″N, 88°20′50″E). Mulberry stem cuttings of S1 cultivar were procured from Matigara Sericulture Complex (26°72′40″N and 88°35′37″E), Siliguri, West Bengal, India.

Preparation and Characterization of Iron Oxide Nanoparticles

Iron nanoparticles were synthesized by adding mature tea leaves extracts (aqueous decoction prepared through refluxing) to 0.01 M $FeCl_3$ (SRL, Batch #T/829638) with a volume ratio of 10:1 at room temperature with continuous uniform stirring for 30 min using magnetic stirrer (REMI EQUIPMENTS). EDTA functionalized iron oxide nanoparticles were prepared by the addition of 25 ml EDTA (0.02 M) with freshly prepared 55 ml iron oxide nanoparticles solution, following the method of Magdalena et al. (2018). The formed particles were removed from reaction medium through precipitation using a strong external magnet and were rinsed thrice with double distilled water and 95% ethanol. After washing, the particles were dehydrated using a hot air oven (Lab Instruments, India, Model-0949) at 65 °C until complete drying.

Characterization of nanoparticles was initially done using UV–Vis spectrophotometer (SYSTRONICS-2201). The size and morphology of the synthesized iron oxide nanoparticles were investigated on a PHILIPS CM 200 transmission electron microscope (TEM). Hydrodynamic size was also measured using dynamic light scattering (DLS) through ZETASIZER NANO ZS90 ZEN3690. The crystalline structure and phase purity of the biosynthesized particles were determined with the help of XRD analysis using a BRUKER AXS D8 ADVANCE (BRUKER KAPPA APEX II).

Experimental Design

The pot experiment was conducted using plastic zipper bag in Mulberry germplasm garden (26°42′34″N and 88°21′06″E, altitude 400 feet) of Department of Botany, University of North Bengal, Siliguri, West Bengal, India in the period of January-June, 2019. Agro-climatic data as collected in that period were average temperature range of about 17.35 °C–23.23 °C, average precipitation of 170.33 mm, average moisture content of 69.16%, normal wind speed of 7.5 Kmph and sun exposure duration of 240.75 h.

Soils after collection from mulberry germplasm garden were air dried and sieved through a 2 mm mesh to get soils of uniform size. According to soil analysis prior to plantation, pH, electrical conductivity (EC), bulk density and moisture content of soil was measured as 4.5, 26.5 µS/cm, 1.25 g/cm^3 and 14.33%, respectively and soil texture was evaluated as sandy loam. Some other biochemical attributes of the tested soil as noted was 1.35%, 2.32%, 0.11%, 22 ppm, 55.43 ppm and 38 ppm for organic carbon, organic matter, available nitrogen, available phosphorus, available potassium and available sulphur, respectively.

The experiment was carried out with six treatments in randomized complete block design with 20 replications of each. Treatment plots were sufficiently spaced for minimizing adjacent influences. Among them, 10 plants were used for above ground growth analysis and 3 plants were sacrificed at each time of evaluation for measuring underground root attributes, biomass analysis along with determination of antioxidant attributes. Treatments were control (distilled water, abbreviated as Con), ferrous sulphate at 10 mg/kg soil dose (abbreviated as FeSO4), iron oxide nanoparticles at two different dosage of 10 mg/kg soil (FeNP 10) and 50 mg/kg soil (FeNP 50) and EDTA functionalized iron oxide nanoparticles at 10 and 50 mg/kg soil dosage (symbolized as FeNP EDTA 10 and FeNP EDTA 50). Each pot (inside length: 10.5 cm, breadth: 7.5 cm and height: 19 cm) was filled with 1.25 kg of soil and the different treatments in solution form were applied to the respective pots. Mulberry stem cuttings after collection was obliquely cut under water and these obliquely cut stem cuttings of equal length (20 cm each) was planted inside pot. Soil application was done initially after plantation (one time) and foliar applications were done by spraying at 30th, 45th and 60th days after plantation at the rate of 5 ppm (for FeNP 10 and FeNP EDTA 10) and 10 ppm (for FeNP 50, FeNP EDTA 50 and FeSO4).

Growth Parameters Evaluation

Best ten plants (replicates) from each treatment were selected to estimate growth parameters of treated mulberry stem cuttings. Leaf length, leaf breadth, maximum shoot length, root lengths were measured using a centimeter scale at 30, 45, 60 and 75th days after plantation. For estimation of shoot biomass and root growth, three plants from each treatment at each time (30, 45, 60 and 75th days after plantation) were harvested, washed with tap water three times and again washed thoroughly with deionized water to remove impurities absorbed on the surface of plant parts. Root growth was evaluated specifically in terms of maximum root length, root branching number and root biomass. Fresh weight of shoots and roots were measured using digital weight balance (QUINTIX 224-10 IN, Sartorius Lab Instruments GmbH & Co. KG). Spouting percentages were calculated using following formula:

$$\text{Sprouting percentage} = \left[(\text{number of buds sprouted}/\text{number of buds present during plantation}) \times 100\right].$$

Biochemical Evaluation

Leaves sample from each treatment (three replication) was collected at 30th, 45th, 60th and 75th after plantation, crushed in cold condition according to the respective methodology, centrifuged and biochemical analysis were performed.

Estimation of Chlorophyll Content

Chlorophyll was extracted in 80% acetone and the amount of total chlorophyll was estimated by standard method described by Arnon (1949).

Estimation of Total Protein Content

Total protein content was estimated following the methodology given by Lowry et al. (1951). The blue-colored complex was formed after well mixing 5 ml alkaline copper solution and Folin-ciocalteu reagent (FCR) with 1 ml protein sample and the absorbance was measured at 660 nm.

Estimation of Total Carbohydrate (Soluble Sugars) and Reducing Sugar Content

0.1 gm of leaf samples were crushed in 10 ml of 80% hot ethanol and filtered using filter paper. After evaporation of existing ethanol by heating the sample, final volume of filtrate was made up to 10 ml by adding distilled water.

Total soluble sugars content was determined by Anthrone method (Thimmaiah 2004). Intensity of resultant blue color

mixture was measured at 620 nm. Using sucrose standard curve, total soluble sugar present in the extract was calculated.

DNSA method (Sadasivam and Manickam 1996) was used for reducing sugar estimation. To 1 ml alcohol free extract, 1 ml DNSA reagent was mixed and incubated in a water bath for 5 min. After the development of the colored product, 1 ml 40% Rochelle salt solution was added and mixed well and absorbance was read at 510 nm.

Estimation of Total Phenol Content

Method prescribed by Kadam et al. (2013) was followed for estimating total phenol content with slight modifications. For estimating, 95% ethanol, 5 ml distilled water, 50% Folin–ciocalteau reagent and 5% Na_2CO_3 was added to 1 ml sample extract and incubated for 1 h. Absorbance was measured at 725 nm and phenol content was estimated using Gallic acid standard curve.

Estimation of Ortho-Dihydric Phenol

Ortho-dihydric phenol was estimated according to the method prescribed by Mahadevan and Sridhar (1986). Arnow's reagent (0.5 ml), 5 ml distilled water and 1 ml 1(N) NaOH was added to 0.5 ml methanolic extract of the sample. Ortho-phenol content was calculated concerning Catechol as standard and the absorbance of the reaction mixture was taken at 515 nm.

Estimation of Flavonoid Content

Flavonoid content was estimated following the method of Atanassova et al. (2011). To 0.5 ml extract, 4 ml distilled water, 5% $NaNO_2$, 10% $AlCl_3$ and 2 ml 1(M) NaOH was added and the absorbance was taken at 510 nm. Flavonoid content was estimated using standard curve prepared from Quercetin.

Study of Antioxidant Enzyme Activity

For estimation of antioxidant enzymes, leaf samples from each treatment (three replicates) were collected at 30th, 45th, 60th and 75th days after plantation. Liquid nitrogen mediated cryo-crushing was done followed by cold centrifugation and the supernatant was used for further analysis.

Estimation of Catalase (CAT) Activity

CAT (EC 1.11.1.5) activity was measured according to Hasanuzzaman et al. (2011). To 40 µl of enzyme, H_2O_2-Potassium phosphate buffer (1:2) combination was mixed and decomposition of hydrogen peroxide was monitored at 240 nm. Enzyme activity was expressed as unit mg protein^{-1} (1 unit = mmole H_2O_2 reduced per minute) using extinction coefficient of 39.4 M^{-1} cm^{-1}.

Estimation of Peroxidase (POD) Activity

POD (EC 1.11.1.7) enzyme activity was determined using the method of Rani et al. (2004). To 3 ml of pyrogallol solution, 1 ml of the enzyme extract was added and the spectrophotometer was adjusted to read 0 at 430 nm. H_2O_2 (0.5 ml) was directly added to the test cuvette and mixed well. The change in absorbance was recorded every 30 s up to 3 min. One unit of peroxidase is defined as the change in absorbance per minute at 430 nm and was expressed as U.ml^{-1}.

Estimation of Polyphenol Oxidase (PPO) Activity

PPO (EC 1.14.18.1) was estimated according to the method given by da Silva and Koblitz (2010) with some modifications. The reaction mixer contains 2.5 ml of potassium phosphate buffer (0.1 M, pH 6.5), 0.3 ml catechol solution (0.01 M) and 0.2 ml of enzyme extract. Absorbance was taken at 495 nm after 5 min of reaction. Activity was expressed as U.ml^{-1}, where one unit of PPO was defined as the amount of enzyme required for increasing unit absorption of the reaction mixture in each minute.

Estimation of Glutathione Reductase (GR) Activity

GR (EC 1.6.4.2) activity was measured by Hasanuzzaman et al. (2011). The reaction mixture comprising 2.7 ml potassium phosphate buffer (0.1 M, pH 7.8), 1 mM EDTA (prepared within buffer), 0.1 ml of NADPH solution (0.2 mM) and 1.0 ml of enzyme source. The reaction was initiated by adding 0.1 ml of GSSG (Glutathione disulphide, 1 mM) and decrease in absorbance due to NADPH oxidation was recorded at 340 nm for 1 min. Activity was expressed as unit (U) (1U = µmol NADPH oxidized per minute) per milligram protein using an extinction coefficient of 6.2 mM^{-1} cm^{-1}.

Estimation of Glutathione S-Transferase (GST) Activity

With slight modifications, spectrophotometric method prescribed by Hasanuzzaman et al. (2011) was followed for determination of GST (EC 2.5.1.18) activity. The reaction mixer contained 2.7 ml Tris HCl buffer (100 mM, pH 6.5), 1 mM GSH, 1 mM 1-chloro-2, 4-dinitrobenzene (CDNB) and 100 µl of enzyme solution. The reaction was initiated by the addition of CDNB and the increasing absorbance was recorded for 1 min at 340 nm. Extinction coefficient of 9.6 mM^{-1} cm^{-1} was used to calculate the enzyme activity.

Estimation of NADPH Oxidase (NOX) Activity

Determination of NOX (EC 1.6.3.1) was done by adding 0.4 ml of enzyme extract to the 2 ml of Tris HCl buffer containing 0.5 mg/ml NBT and 134 mM NADPH and absorbance was taken at 470 nm. Extinction coefficient of 21.6 mM^{-1} cm^{-1} was used to calculate enzyme activity (Zhang et al. 2018).

Data Analysis and Program Used

Data of 10 replicates were collected for evaluation of morphological attributes and results were expressed as mean ± standard deviation (SD), however for plant biomass, root growth, biochemical and antioxidant enzymes parameters evaluation, three replicates were taken. Tests of statistical differences were carried out by Tukey's Honestly Significant Difference (HSD) test at $p \leq 0.05$, where the treatments differ significantly were denoted with different letters (a, b, c etc.). Excel macros DSAASTAT, version 1.022 (DSAA, Italy) extension has been used to calculate this. Principal component analysis (PCA) and heat map was performed based on 75th day's data different variables and treatments under study. PCA analysis was carried out using web enabled Clustvis program (Metsalu and Vilo 2015) and to make biplots first two components (PC1 and PC2) were used. Heat map was prepared using web enabled Heatmapper (Babicki et al. 2016) based on Pearson distance measurement method by preparing percentile rank.

Results and Discussion

Characterization of Iron Oxide Nanoparticles

Color change of ferric chloride solution, from pale yellow to dark black, was the first and foremost indication of nanoparticles synthesis. However, formation was confirmed by UV–Visible spectra analysis, showed absorption maxima at 254 nm (Fig. 1a), which is in agreement with the previous findings (Vadivel et al. 2012; Eslami et al. 2018). TEM images (Fig. 1b) confirmed that formed nanoparticles are of spherical in shape with an average size of 13.10 nm. However, the hydrodynamic size obtained through DLS

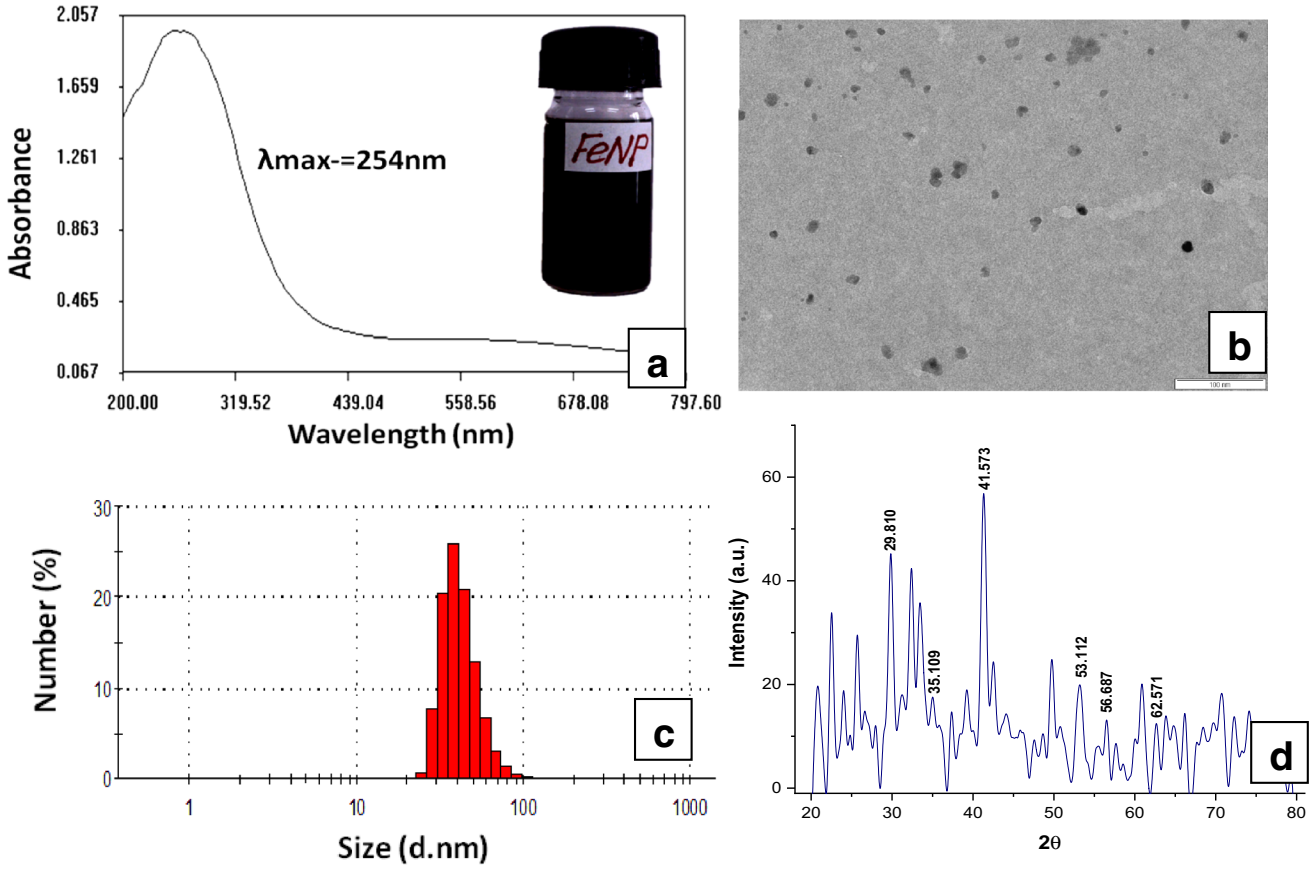

Fig. 1 Characterization of biosynthesized iron oxide nanoparticles, **a** UV–visible spectra analysis, **b** transmission electron micrograph (TEM), **c** dynamic light scattering (DLS), **d** X-ray diffraction (XRD) analysis

(Fig. 1c) is quite higher (59.24 nm) than the size acquired through TEM. XRD analysis showed prominent peaks at 29.81°, 35.10°, 41.57°, 53.11°, 56.69°, 62.57° corresponding to (hkl) values of (220), (311), (400), (422), (511), (440) Bragg's reflections plane (Fig. 1d). The obtained peaks match with existing standard JCPDS library (card no 39-1346), representing standard cubic structure of γ-Fe_2O_3 (maghemite) nanoparticles. However, as some extra small peaks were also appeared in the obtained XRD spectra, it could be the magnetite or other form of iron oxide nanoparticles or rather to say it might be the mixture of different phase of iron oxide nanoparticles. Average crystalline size of the formed nanoparticles was calculated using Debye–Scherrer's equation and was found to be 11.98 nm, which was in close proximity with the average particle diameter obtained through TEM analysis.

Effect of Iron Oxide Nanoparticles on the Sprouting Percentage and Days to Appear First Leaf

Mulberry stem cuttings responded variably towards different concentrations of normal and EDTA functionalized iron oxide nanoparticles. As shown in Table 1, application of both the iron oxide nanoparticles and its chelated form significantly improved sprouting percentage and also helped to reduce the days to appear first leaf. Results of sprouting percentage showed a clear statistical differentiation among different concentrations of iron oxide nanoparticles and its EDTA functionalized form. FeNP EDTA 50 showed almost 82% sprouting percentage which was 166% improvement over control. Iron nanoparticles showed a noteworthy response in quick appearance of leaves. Cuttings treated with FeNP 10 took only twelve days to appear its first leaf in comparison to control which took almost twenty-seven days.

Effect of Iron Oxide Nanoparticles on the Growth Parameters

The phenotypic traits of plants showed dramatic effects on the resulting plants' growth and development upon exposure to the FeNPs treatments. The plants exposed to FeNPs-EDTA have significantly longer shoots and bigger leaves in comparison to the control and plants treated with normal iron salt supplementation ($FeSO_4$). The morphological appearance of the treated plants is presented in Fig. 2a. Results pertaining to shoot height showed that maximum increase in height of about 78.28% by FeNP EDTA 50 treatments at 75th days after plantation against control. This result

Table 1 Effect of iron oxide nanoparticles and EDTA functionalized iron oxide nanoparticles on the sprouting percentage and days to appear first leaves of Mulberry

Parameters	Treatments					
	FeNP10	FeNP EDTA 10	FeNP 50	FeNP EDTA 50	FeSO4	Control
Sprouting percentage (%)	45.39 ± 1.03^{e}	63.44 ± 1.16^{d}	73.43 ± 0.78^{b}	81.47 ± 1.16^{a}	66.66 ± 1.32^{c}	30.52 ± 0.80^{f}
Days required for appearing first leaf	10.33 ± 1.16^{d}	14.67 ± 1.21^{c}	13 ± 1.09^{c}	14.5 ± 1.04^{c}	20.33 ± 1.03^{b}	27.83 ± 1.16^{a}

Results are expressed as mean ± SD, n = 10. Values with different letters (a, b, c etc.) differ significantly at $p \leq 0.05$ by Tukey's Honestly Significant Difference (HSD) test

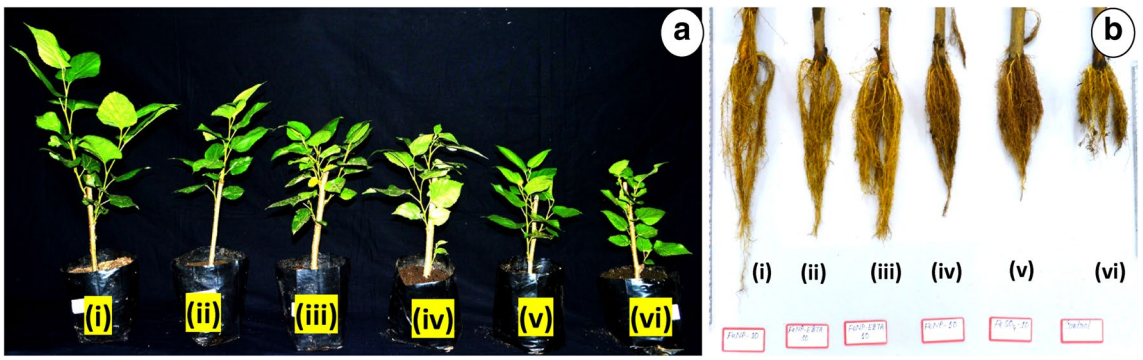

Fig. 2 Effect of iron oxide nanoparticles EDTA functionalized iron oxide nanoparticles on morphological appearance and root growth (**a** and **b**). For morphological appearance of the plant: (i) FeNP EDTA 50, (ii) FeNP 10, (iii) FeNP 50, (iv) FeNP EDTA 10, (v) FeSO4, (vi) Control. For root appearance: (i) FeNP10, (ii) FeNP EDTA 10, (iii) FeNP EDTA 50, (iv) FeNP 50, (v) FeSO4, (vi) Control

is in conformity with Ju's study (Ju et al. 2019); where they showed that 20 nm size ranged iron oxide nanoparticles-EDTA conjugate had positive growth potential in *Lepidium sativam*. Yuan et al. (2018) also reported significant influence of iron oxide nanoparticles on plant height in comparison to control and Fe^{2+} ions treatment. From Table 2 it was observed that both the nano-micronutrient fertilizer was effective in escalating the number of leaves per plants. After 75th days of plantation, the highest number of leaves belongs to the cuttings treated with FeNP 10 which showed an increment of 52.73% over control. Cuttings exposed to FeNP EDTA 50 had 53.48% larger leaf area compared to the non-treated groups (control). Yoon et al. (2019) reported similar sorts of results where they found 53% leaf area increment on application of nanoscale zero valent iron (nZVI) nanoparticles. No significant changes were observed in branching number in iron oxide nanoparticles treated cuttings compared to control. According to Elanchezhiana et al. (2017), application of Fe_3O_4 nano-micronutrient in maize significantly improved shoot length, leaf area, root and shoot dry biomass and other biochemical parameters. Both maximum shoot length and average number of branching showed optimum value at FeNP EDTA 50 at final day of observation (75th day after plantation) shared a ratio of 4.20:1. On the other hand at the same dose maximum shoot length and number of leaves showed almost 1:1 ratio. Increment of growth attributes can be explained by high level of photo assimilates synthesis and accumulation. Photo-assimilates plays central role in plant growth, development (Allsopp 1954), flowering (Kraus and Kraybill 1918) and apical dominance (Loeb 1924). Small sugars were considered as important in signaling pathway of plants (Moore et al. 2003). Ende (2014) speculated that, internal sugar/IAA proportion within the buds or within the adjoining stem may somehow be connected prior to initiation of bud outgrowth. Sprouting percentage increment, early leaf appearance and evenness in branching number depicted not only the accumulation but also the effective mobilization of photo-assimilates. Increase in leaf area recorded in our study in association with better utilization of iron oxide nanoparticles might be a kind of adaptation towards proficient photosynthesis as stated by Fernández et al. (2008).

Figure 2b represents the root appearance of treated mulberry cuttings after 75 days of plantation. Both FeNP and FeNP EDTA showed a noticeable change on the development of roots over control and normal iron salt supplementation (Table 3). A prominent increase in root length and root branching number was observed in low concentration of both

Table 2 Effect of iron oxide nanoparticles and EDTA functionalized iron oxide nanoparticles on different growth parameters of Mulberry at different growth stage

Attributes	Days after plantation	Treatments					
		FeNP10	FeNP EDTA 10	FeNP 50	FeNP EDTA 50	$FeSO_4$	Control
Maximum shoot length (cm)	30th Days	6.08 ± 0.45^{a}	6.61 ± 0.44^{a}	7.10 ± 0.34^{a}	7.47 ± 0.48^{a}	4.03 ± 0.46^{b}	3.25 ± 0.31^{b}
	45th Days	7.99 ± 0.61ab	8.25 ± 1.11^{ab}	8.55 ± 0.94^{a}	9.23 ± 1.04^{a}	5.55 ± 0.76^{bc}	5.06 ± 0.64^{c}
	60th Days	15.09 ± 1.48^{a}	11.70 ± 2.71^{abc}	11.97 ± 2.63^{abc}	13.96 ± 1.29^{ab}	8.07 ± 1.18^{bc}	6.07 ± 0.51^{c}
	75th Days	16.49 ± 1.64^{b}	14.31 ± 1.81^{b}	16.18 ± 1.45^{b}	20.20 ± 2.07^{a}	12.86 ± 1.89^{b}	11.33 ± 0.65^{b}
Number of leaves per plant	30th Days	9.80 ± 0.63^{b}	$10.60 \pm 0.84a^{b}$	10.40 ± 0.69^{ab}	$11.10 \pm .073^{a}$	6.90 ± 0.31^{c}	5.87 ± 0.64^{c}
	45th Days	11.70 ± 1.33^{b}	$12.00 \pm 1.05a^{b}$	12.40 ± 0.96^{ab}	13.80 ± 1.13^{a}	8.40 ± 1.17^{c}	6.66 ± 1.11^{c}
	60th Days	18.7 ± 1.49^{a}	16.9 ± 1.37^{abc}	15.7 ± 1.88^{bc}	18.2 ± 1.68^{ab}	14.7 ± 1.33^{cd}	12.11 ± 1.69^{d}
	75th Days	22.3 ± 1.41^{a}	19.3 ± 1.15^{bc}	17.2 ± 1.13^{cd}	20.4 ± 1.5^{ab}	16.9 ± 1.37^{de}	14.6 ± 0.84^{e}
Average leaf length (cm)	30th Days	3.22 ± 0.22^{bcd}	3.42 ± 0.21^{bc}	3.54 ± 0.19^{ab}	3.87 ± 0.17^{a}	3.10 ± 0.19^{cd}	2.90 ± 0.15^{d}
	45th Days	4.23 ± 0.18^{b}	4.54 ± 0.15^{a}	4.48 ± 0.14^{ab}	4.67 ± 0.13^{a}	4.48 ± 0.19^{ab}	3.40 ± 0.16^{c}
	60th Days	4.50 ± 0.15^{b}	4.80 ± 0.18^{ab}	4.94 ± 0.221^{a}	4.96 ± 0.19^{a}	4.72 ± 0.18^{ab}	3.9 ± 0.13^{c}
	75th Days	5.23 ± 0.24^{a}	5.32 ± 0.21^{a}	5.45 ± 0.19^{a}	5.36 ± 0.15^{a}	4.97 ± 0.16^{a}	4.30 ± 0.24^{a}
Average leaf breadth (cm)	30th Days	2.45 ± 0.22^{bcd}	2.60 ± 0.21^{abc}	2.70 ± 0.19^{ab}	2.90 ± 0.17^{a}	2.35 ± 0.19^{cd}	2.12 ± 0.15^{d}
	45th Days	2.90 ± 0.18^{bc}	3.10 ± 0.15^{ab}	3.15 ± 0.14^{ab}	$3.28 \pm 0.13a$	2.89 ± 0.19^{bc}	2.67 ± 0.16^{c}
	60th Days	3.60 ± 0.15^{c}	3.98 ± 0.18^{ab}	4.15 ± 0.221^{ab}	4.29 ± 0.19^{a}	3.87 ± 0.18^{bc}	3.65 ± 0.13^{c}
	75th Days	3.82 ± 0.24^{bc}	4.10 ± 0.21^{ab}	4.19 ± 0.19^{ab}	4.36 ± 0.15^{a}	3.98 ± 0.16^{b}	3.54 ± 0.24^{c}
Average number of branching	30th Days	2.70 ± 0.48^{a}	2.88 ± 0.78^{a}	2.80 ± 0.42^{a}	2.90 ± 0.73^{a}	2.66 ± 0.74^{a}	2.33 ± 0.86^{a}
	45th Days	3.16 ± 0.40^{a}	3.00 ± 0.78^{a}	3.00 ± 0.66^{a}	3.00 ± 0.92^{a}	2.87 ± 064^{a}	2.62 ± 0.51^{a}
	60th Days	3.40 ± 0.51^{a}	3.20 ± 0.42^{a}	$3.50 \pm .52^{a}$	3.39 ± 0.95^{a}	3.40 ± 0.51^{a}	3.00 ± 0.5^{a}
	75th Days	3.90 ± 0.73^{a}	3.55 ± 0.69^{a}	3.90 ± 0.56^{a}	4.20 ± 0.78^{a}	3.60 ± 0.69^{a}	3.40 ± 0.84^{a}

Results are expressed as mean ± SD, n = 10. Values with different letters (a, b, c etc.) differ significantly at $p \leq 0.05$ by Tukey's Honestly Significant Difference (HSD) test

Table 3 Effect of iron oxide nanoparticles and EDTA functionalized iron oxide nanoparticles on maximum root length and branching number of Mulberry at different growth stage

Attributes	Days after plantation	Treatments					
		FeNP10	FeNP EDTA 10	FeNP 50	FeNP EDTA 50	FeSO4	Control
Maximum root length (cm)	30th Days	6.20 ± 0.20^{a}	5.80 ± 0.10^{ab}	4.90 ± 0.14^{c}	$5.50 \pm 0.20b^{c}$	4.20 ± 0.10^{b}	3.17 ± 0.35^{e}
	45th Days	22.11 ± 1.44^{a}	13.15 ± 1.13^{b}	11.72 ± 0.63^{bc}	12.57 ± 0.60^{b}	10.87 ± 0.418^{bc}	8.77 ± 0.61^{c}
	60th Days	26.88 ± 1.4^{a}	16.8 ± 1.21^{b}	15.21 ± 1.05^{bc}	15.32 ± 1.47^{bc}	14.59 ± 0.79^{bc}	11.85 ± 0.5^{c}
	75th Days	28.88 ± 1.17^{a}	23.66 ± 1.76^{ab}	21.79 ± 1.67^{bc}	21.26 ± 2.08^{bc}	20.04 ± 1.57^{bc}	16.96 ± 1.60^{c}
Average root branching number	30th Days	69.33 ± 2.52^{a}	60.33 ± 2.08^{bc}	64.00 ± 1.00^{ab}	65.33 ± 1.53^{ab}	54.00 ± 2.00^{c}	44.33 ± 2.52^{d}
	45th Days	84.67 ± 1.52^{a}	74.00 ± 1.00^{bc}	71.00 ± 2.00^{bc}	76.33 ± 1.52^{b}	69.00 ± 1.00^{c}	61.76 ± 3.21^{d}
	60th Days	94.67 ± 1.52^{a}	87 ± 2^{bc}	88.67 ± 1.52^{abc}	91.33 ± 2.52^{ab}	83 ± 2.64^{c}	75.67 ± 2.51^{d}
	75th Days	118.67 ± 6.65^{a}	99.33 ± 3.21^{bc}	106 ± 3^{ab}	107 ± 3.6^{ab}	97.67 ± 5.03^{bc}	88 ± 3^{c}

Results are expressed as mean ± SD, n = 3. Values with different letters (a, b, c etc.) differ significantly at $p \leq 0.05$ by Tukey's Honestly Significant Difference (HSD) test

FeNP and FeNP-EDTA, supports the findings of Palchoudhury et al. (2018). On evaluating root branching number, it was found that except FeNP 10, there was no significant difference among different dosage of iron oxide nanoparticles and EDTA functionalized iron oxide nanoparticles. Maximal significant root length improvement was recorded in FeNP 10 after 75th days of plantation which showed almost 34% of increment over control. Formation of adventitious roots in cuttings is governed by various morphological and physiological processes and generally triggered by several external factors including mineral nutrition. Previous studies by various researchers have indicated the accumulation of several micronutrients including iron and copper at the base of stem cuttings (Svenson and Davies 1995; Rowe et al. 1999). Iron specifically acts locally in the meristematic cells of adventitious root primordia and enhances root growth by promoting cell division (Hilo et al. 2017). Roschzttardtz et al. (2011) observed a high accumulation of iron in nucleolus of plant cells, suggesting the possible involvement of this element in ribosomal RNA biosynthesis. Indeed, biogenesis of ribosome appears to be correlated with rate of cell proliferation, which is becoming a vital factor in actively dividing cells (Manzano et al. 2013). In this study, on application of iron oxide nanoparticles externally, maximum length of the root and its branching number showed utmost value at FeNP 10 dosage with a ratio of 1:4.10, which is almost similar to the ratio of shoot branching number and maximum shoot length. Enhanced root length and branching number helps in proper succession of cuttings as adventitious root formation is a prerequisite for the vegetative propagation in horticulture, agriculture and forestry (Hartmann et al. 2011). Higher numbers of roots observed in present study help the plants to access more water and nutrients (Khan et al. 2012). In fact, high water availability assists plants to maintain cell turgidity (Majeed et al. 2020). Turgid cells enhanced the leaf size to harvest more light which ultimately increased yield and biomass of the plants (Zayed et al. 2011).

Evaluation of plant biomass is a primary criterion in the study of functional plant biology which might predict the resource capture, usages and bioavailability of a plant

Table 4 Effect of iron oxide nanoparticles and EDTA functionalized iron oxide nanoparticles on biomass of Mulberry at different growth stage

Attributes	Days after plantation	Treatments					
		FeNP10	FeNP EDTA 10	FeNP 50	FeNP EDTA 50	FeSO4	Control
Fresh weight of shoot biomass (gm)	30th Days	$2.730 \pm .100^{b}$	3.150 ± 0.120^{a}	3.510 ± 0.055^{a}	2.1788 ± 0.100^{c}	1.940 ± 0.150^{c}	1.940 ± 0.138^{c}
	45th Days	4.470 ± 0.100^{b}	4.330 ± 0.152^{b}	4.150 ± 0.050^{b}	5.100 ± 0.100^{a}	3.530 ± 0.152^{c}	2.760 ± 0.145^{d}
	60th Days	5.340 ± 0.141^{b}	5.310 ± 0.172^{b}	5.150 ± 0.081^{b}	6.330 ± 0.019^{a}	4.640 ± 0.231^{c}	3.530 ± 0.126^{d}
	75th Days	6.380 ± 0.276^{a}	6.640 ± 0.229^{a}	6.650 ± 0.170^{a}	7.010 ± 0.106^{a}	5.600 ± 0.206^{b}	4.650 ± 0.304^{c}
Fresh weight of root Biomass (gm)	30th Days	1.110 ± 0.085^{a}	0.860 ± 0.030^{b}	$0.650 \pm 0.041c$	0.830 ± 0.052^{b}	0.540 ± 0.047^{c}	0.170 ± 0.038^{d}
	45th Days	1.700 ± 0.070^{a}	1.530 ± 0.030^{b}	1.230 ± 0.050^{c}	1.540 ± 0.040^{b}	0.710 ± 0.014^{d}	0.500 ± 0.019^{e}
	60th Days	1.940 ± 0.052^{a}	1.720 ± 0.047^{bc}	1.640 ± 0.038^{c}	1.800 ± 0.008^{b}	1.080 ± 0.049^{d}	0.970 ± 0.032^{d}
	75th Days	2.340 ± 0.020^{a}	2.110 ± 0.066^{b}	1.900 ± 0.034^{c}	1.940 ± 0.040^{c}	1.510 ± 0.030^{d}	1.230 ± 0.040^{e}

Results are expressed as mean ± SD, n = 3. Values with different letters (a, b, c etc.) differ significantly at $p \leq 0.05$ by Tukey's Honestly Significant Difference (HSD) test

(Wilson et al. 1999; Poorter and Nagel 2000). The obtained results for mean fresh biomass (shoot and root) of various treatments were presented in Table 4. The obtained results for mean fresh shoot and root biomass of two different dosages of both the iron oxide and EDTA functionalized iron oxide nanoparticles showed no significant variation among them; however, exhibited an increased value over control and ferrous sulphate treated cuttings. As a whole, application of iron nanoparticles at the rate of 10 mg/kg soil (FeNP 10) has resulted in improvement of both shoot and root fresh biomass of the cuttings by 37% and 90% respectively in comparison with control. With increasing days after plantation, shoot and root biomass at optimum dose (FeNP EDTA 50 for shoot and FeNP 10 for root) showed a positive correlation ($r^2 = 0.778$) sharing a ratio of 3:1. In soybean crops, it was established that magnetite nanoparticles were able to increase the leaf and pod dry weights (Sheykhbaglou et al. 2010). Askary et al. (2017) reported that iron nanoparticles treatment on *Mentha piperita* L. under salinity stress increased fresh and dry weight values as compared to control. Enhancement of biomass by application of iron oxide nanoparticles can be correlates with improved chlorophyll production, as photosynthesis is the most crucial process for plant growth, development and biomass production (Raines 2011; Khan et al. 2017). Root length, branching number and its succession may also played a stimulatory role in plant biomass improvement as reported by Zhang et al. (2017) who showed a positive correlation between shoot biomass and root length density. Improvement in leaf area and plant height may also be the driving force in plant biomass increment (Majeed et al. 2020).

Effect on Biochemical Content

Besides biomass improvement, iron oxide nanoparticles treatment significantly enhanced leaf chlorophyll content over control as well as normal iron supplementation; however, there was no significant variation among different concentrations of iron oxide and EDTA functionalized iron oxide nanoparticles (Fig. 3). Compared with control, chlorophyll content was found to be higher in *Capsicum annuum* treated with 0.05 mM/L iron nanoparticles (Yuan et al. 2018). Alfalfa grown in nanoscale zero valent iron (nZVI) amended soil contained more chlorophyll than control and normal Fe-EDTA treated groups (Kim et al. 2019). In plants iron acts as a key element playing vital role in electron transfer process to operate photosynthetic system (López-Millán et al. 2016). Typically, in photosynthetic cells 80% of iron is found to be involved in the synthesis of cytochrome and other heme containing molecules as well as chlorophyll and construction of Fe-S clusters (Briat et al. 2007). Both chlorophyll a and chlorophyll b are helpful in absorption of light and consequent electron transport mostly enabled by Fe–S protein (Senge et al. 2014). These Fe–S proteins (consisting of Fe–S clusters) through Fe^{+2}/Fe^{+3} oxidation states transfer electrons in photosystem and its role in chlorophyll production are the crucial steps in the process of production of energy in plants, growth and development (Balk and Lobréaux 2005). Previous reports suggest that 30% improvement in photosynthesis can increase 10% relative growth (Kirschbaum 2011). Application of iron oxide nanoparticles enhanced chlorophyll content, possibly by influencing both enzymatic and biochemical activities during photosynthesis (Ghafariyan et al. 2013). In our studies, higher concentration of chlorophyll a relative to chlorophyll b was also observed, which is comparable with the findings reported by Ju et al. (2019).

Protein and sugar content of all the plants increased with increasing days after plantation. Increment rate was higher in plants treated with iron oxide nanoparticles (FeNP) or EDTA functionalized iron oxide nanoparticles (FeNP EDTA) in comparison with control. On the other hand, phenolic content exhibited contrary results, where with increasing days after plantation the phenolics phytochemicals gradually declined. High phenolic contents belonging to the cuttings treated with FeNP EDTA 50, showed improvement of 67.18%, 18.45% and 42.75% over control for total phenol, ortho-dihydric phenol and flavonol, respectively. Enhancement of total phenol content in radish root was recorded by application of combined dosage of zinc oxide and iron oxide nanoparticles (Mahmoud et al. 2019). Lopez-Vargas et al. (2018) also observed improvement of flavonoid content by 36.14% over control by application of copper nanoparticles in tomato plants. Furthermore, the higher initial phenolic content observed in present study attributed to young leaves, buds and young branches, which get matured with increasing days (Raya et al. 2015). Our results was also in conformity with Ghasemzadeh et al. (2014), who showed higher phenolic content in early growth stage of *Clinacanthus nutans* compared to mature one. Except FeNP EDTA 50 treated cuttings, no significant variation among different treatments in sugar content was observed. Application of FeNP EDTA 50 enhanced both total sugar and reducing sugar by 17.99% and 42.29%, respectively, in comparison with control. The final ratio of total soluble sugar and reducing sugar was observed as 127:1. This increase in sugar content is perhaps due to increased rate of photosynthesis and better accumulation of photo-assimilates (Yoon et al. 2019). Tobacco plants treated with 5 nm size ranged Fe_3O_4 nanoparticles have shown an increment in sugar content compared with control and other treated plants (Alkhatib et al. 2019). When *Arabidopsis thaliana* was exposed to nZVI, Yoon et al. (2019) observed significant enhancement of 52%, 27% and 44% of different carbohydrate metabolites like starch, sucrose and glucose content, respectively. However, on iron oxide nanoparticles exposure, Kim et al. (2019) and Wang et al. (2016) reported

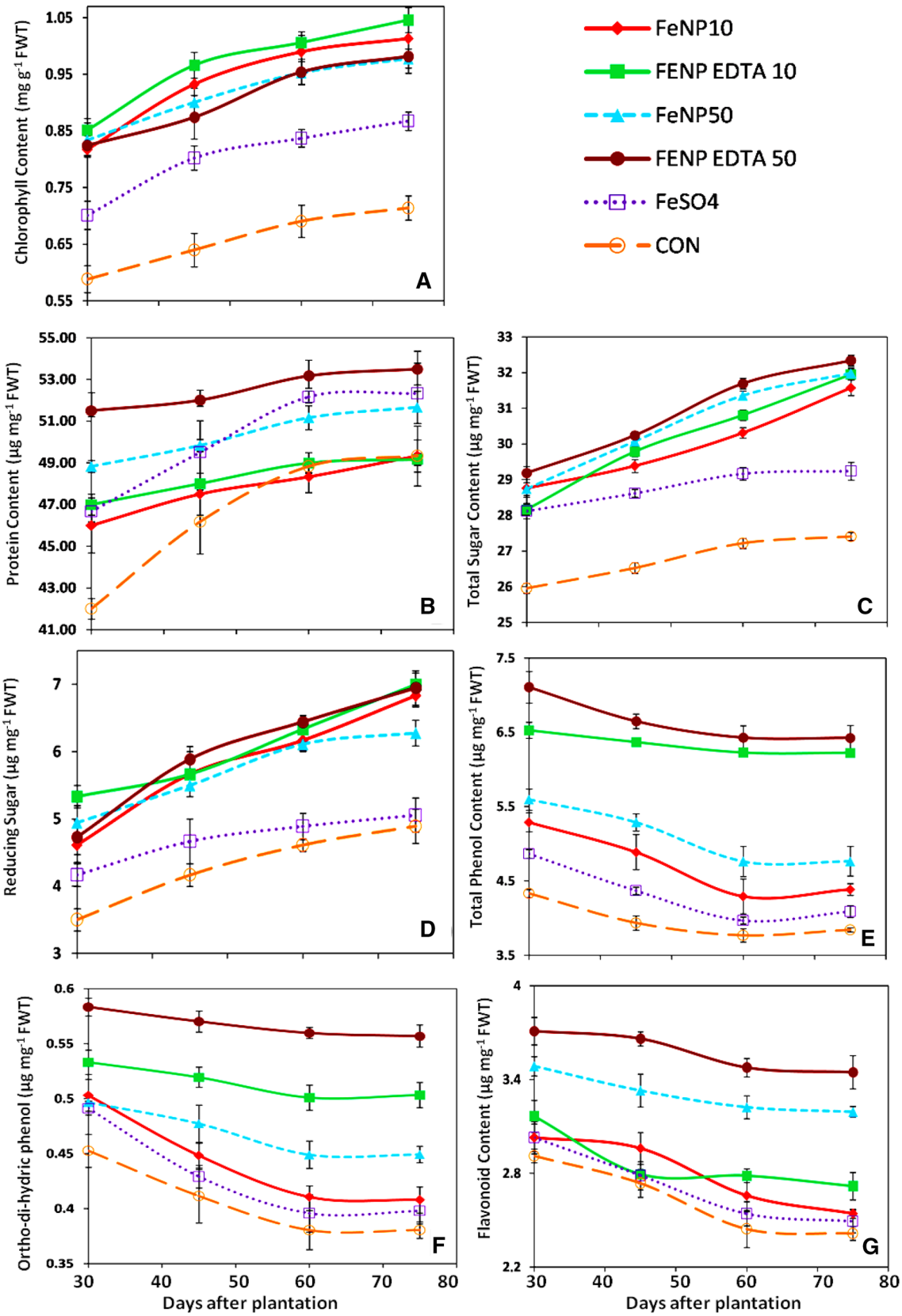

Fig. 3 Effect of iron oxide nanoparticles EDTA functionalized iron oxide nanoparticles on different biochemical parameters, **A** chlorophyll content, **B** total protein content, **C** total sugar, **D** reducing sugar, **E** total phenol, **F** ortho-di-hydric phenol, **G** flavonoid content.Each vertical bar above the means indicates standard deviation of three replicates (n = 3)

no significant changes in sugar accumulation compared with control. Also in current study, no such improvement in protein content was observed except FENP EDTA 50, where only 8% improvement over control was observed which supports the findings of Yoon et al. (2019).

Antioxidant Enzyme Activity

Reactive oxygen species (ROS) is normally generated as a by-product of plant cellular metabolism. When stem cuttings were isolated from main plants, certain mechanical injury was imposed; this caused biotic stress in plants. Antioxidant enzymes and biochemical defense responses are very common under the conditions of wounding (Prasad et al. 2020). A series of local response get activated to repair the damages, which includes deposition of suberin, callose, synthesis of defensive proteins, various phenolics etc. (Savatin et al. 2014). Applying an increasing amount of micro-element is known to affect the efficiency of several antioxidant enzymes which are the major ROS scavenger in plant cells and organs. Nanoparticles primarily interact with plant systems through chemical processes which generate ROS, creates oxidative damage and lipid peroxidation. According to previous reports nanoparticles generally increased the activity of antioxidant enzymes such as CAT, SOD and POD etc. (Laware and Raskar 2014). In our present study, with respect to control, significant consequence of nanoparticles interaction based on exposure time and treatment concentration were observed on the activity of all the studied enzymes (Fig. 4).

Catalase is an important heme containing enzyme in redox cycle (Shigeokaet al. 2002), showed highest activity in the plants treated with FeNP EDTA 10 at 30th DAP and following the trend up to 75th DAP. NOX also followed the same trend with an increment of 2.58-fold over control. In agreement with our observations, Rui et al. (2016) by applying different dosage of maghemite and Fe-EDTA in peanut shoots observed increased CAT activity in all the treatments exceeding control. POD is a heme protein belongs to oxidoreductases which catalyze the oxidation of a wide range of inorganic and organic substances. FeNP EDTA 50 treated plants showed highest activity of POD, which surpassed the control by 71%. In case of PPO and GR, no significant variation among two different dosages of FeNP EDTA was observed. The GST activity of plant tissue increased after exposure with different Fe treatment, being highest in FENP 10, which surpassed control by 81.93%. Control and normal iron salt supplementation ($FeSO_4$) showed no significant variation for GR, CAT and NOX. Activities of all the studied enzymes except POD, however, increased along with the plant growth.

Higher activity of POD, CAT and protein content was observed in mung bean treated with 10 ppm nano iron-chelate which supports our findings. Similar results were also observed by applying nano-Fe oxide in wheat. Ghafari and Razmjoo (2013) observed increased content of chlorophyll, carbohydrate and protein along with higher antioxidant enzyme activities. Through lipid peroxidation assay, Hu et al. (2017) showed excess ROS production in Fe_2O_3 induced *Citrus maxima*, also showed increased production of antioxidant enzymes like CAT and POD. This might have indicated higher production of ROS and thereby increased scavenging potential of ROS to reduce oxidative stress and difficulties in plants. Becana et al. (1998) explained that, in the structures of antioxidant enzymes, shortage of iron as a cofactor leads to lowering the efficacy of antioxidant enzymes and elevating the plant's susceptibility towards environmental stresses. According to Asl et al. (2019), even under optimal condition, different metabolic processes create ROS. This enhanced activity of antioxidant enzymes as observed in our present experiment can increase the tolerance level of plants to oxidative stress (Mittler 2002). By comparing the activities of all the studied enzymes, it is evident that the accumulation of treated particles induced strong antioxidant responses in *Morus alba.*

Understanding Interactions Between Various Treatments and Variables Through PCA and Heatmap-Based Clustering Approach

PCA and Heat map was used to assess the effect of application of different dosage of iron oxide and EDTA functionalized nanoparticles on mulberry propagation, to avail maximum amount of data variability and to draw an interaction between variables and treatments. First two principal components i.e. PC1 (70.37%) and PC2 (18.38%) accounted for a total of 88.75% overall data variability (Fig. 5). On the basis of factor loading values, it was observed that lower right plot mainly represents control and $FeSO_4$ treatments (PC1 loadings are positive but PC2 loadings are negative). Higher concentration of both the iron oxide nanoparticles i.e. FeNP 50 and FeNP EDTA 50 were placed together in the lower left plot with both negative values, indicating a positive correlation. Whereas, FeNP 10 and FeNP EDTA 10 i.e. lower dose of iron oxide nanoparticles occupied the upper left plot (positive factor loadings are associated with second component and negative factor loadings are associated with first component). Presence of these two groups in different plots clearly depicted the concentration dependent effect of both the iron oxide nanoparticles on mulberry. Short distance between control and normal iron salt supplementation ($FeSO_4$) confirmed the rather small impact of $FeSO_4$ on the morpho-physiochemical attributes of mulberry.

PCA of different variables showed two major clusters (Fig. 6). First cluster grouped root attributes (root length, branching number and biomass), number of leaves per

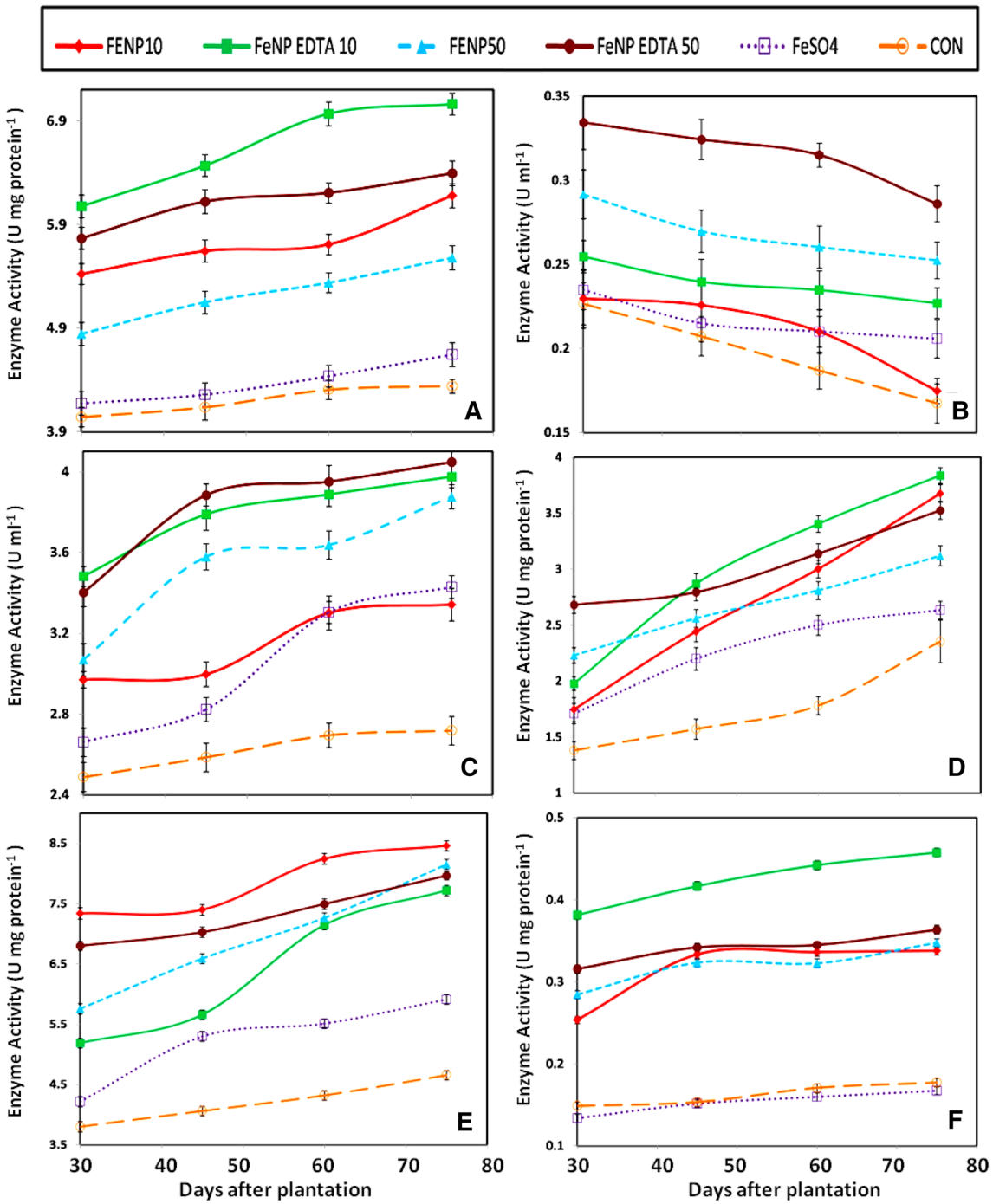

Fig. 4 Effect of iron oxide nanoparticles EDTA functionalized iron oxide nanoparticles on different antioxidant enzymes attribute, **A** catalase, **B** peroxidase, **C** polyphenol oxidase, **D** glutathione reductase, **E** glutathione-s-transferase, **F** NADPH oxidase activity. Each vertical bar above the means indicates standard deviation of three replicates (n = 3)

plant, most of the antioxidant enzymes (catalase, NADPH oxidase, glutathione reductase, glutathione s transferase) along with some biochemical parameters (reducing sugar, chlorophyll). That indicate shoot length, branching number and biomass were positively correlated. Increment of chlorophyll and reducing sugar in plants and placement of these two together in same cluster might be due to increment in photo-assimilates accumulation accelerated with the production of active metabolites like reducing sugar which helps in energy production. Enhancement in active metabolism leads to generation of ROS which ultimately leads to activation of antioxidant enzymes like catalase, glutathione reductase,

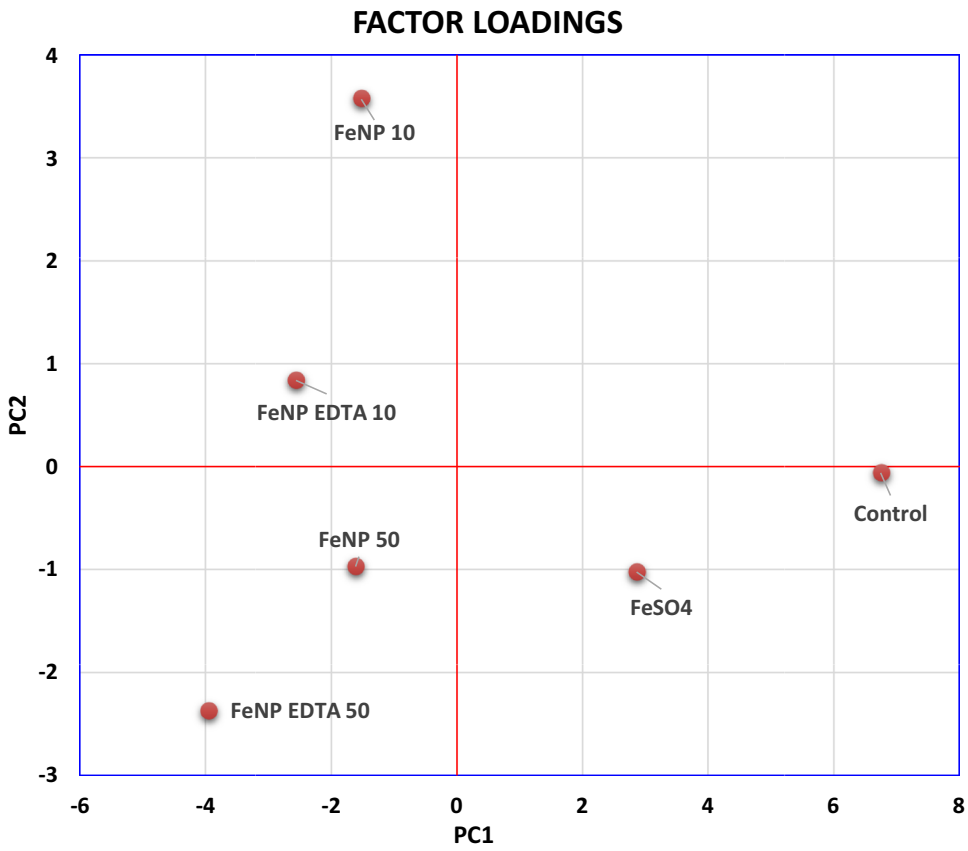

Fig. 5 Ordination diagram as obtained through principal component analysis (PCA), showing similarities between experimental treatments on 75th day dataset of overall variables

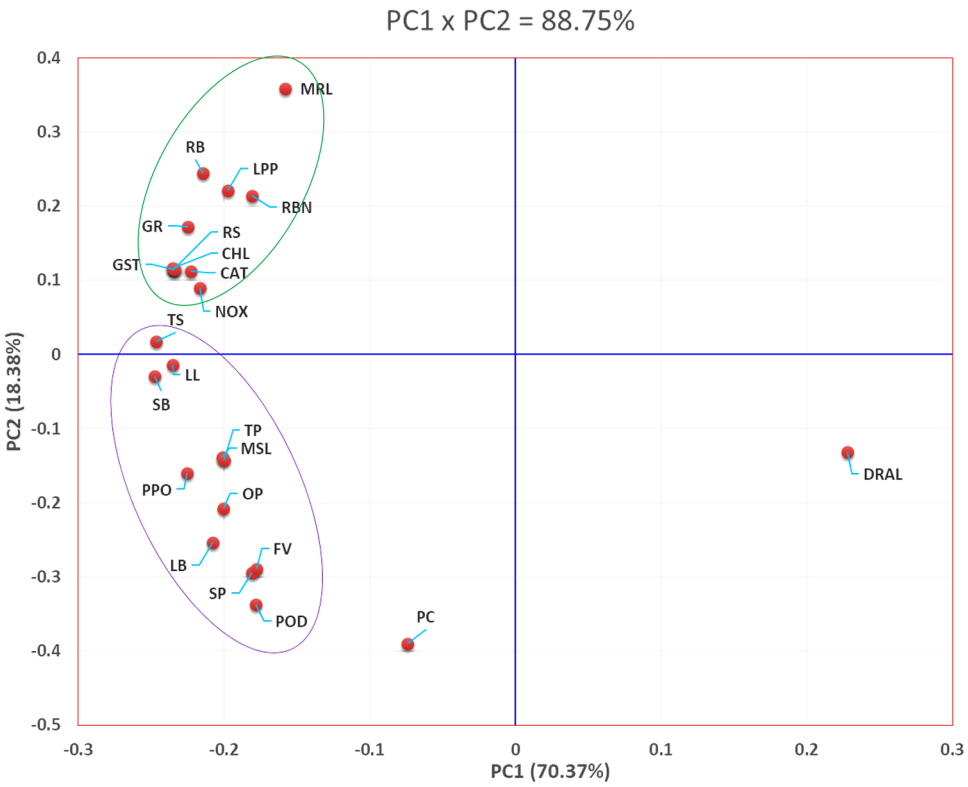

Fig. 6 Ordination diagram as obtained through principal component analysis (PCA), showing similarities between various growth and biochemical attributes, performed using the data of 75th days after plantation *DRAL* days required for appearing first leaf, *PC* protein content, *NOX* NADPH oxidase, *SP* sprouting percentage, *LB* leaf breadth, *POD* peroxidase, *LL* leaf length, *TS* total sugar, *FV* flavonol, *PPO* polyphenol oxidase, *OP* ortho dihydric phenol, *SB* shoot biomass, *TP* total phenol, *GST* glutathione s transferase, *MSL* minimum shoot length, *RBN* root branching number, *CHL* chlorophyll, *GR* glutathione reductase, *RS* reducing sugar, *CAT* catalase, *MRL* maximum root length, *LPP* number of leaves per plant, *RB* root biomass

NADPH oxidase and glutathione-s-transferase. Panda and Sarkar (2012) also showed a significant positive correlation between chlorophyll content and activities of antioxidant enzymes. Another major cluster mainly represents above ground growth parameters together with polyphenols associated with defense system and antioxidant enzymes like polyphenol oxidase and peroxidase. Initially the content of total phenol, ortho di-hydric phenol and flavonol was maximum, which gradually decreases with increasing days after plantation. The reason behind this might be due to the fact that initially the cuttings were susceptible to environmental stresses which gradually got acclimatized with increasing days after plantation. The enzyme peroxidase, using phenols played role in oxidative stress mitigation. Polyphenol oxidase also converts polyphenols to quinones group of compounds to facilitate defense system (Taranto et al. 2017). Heatmap is another data visualizing technique used, in which treatment and variables were arranged in row and column, respectively (Fig. 7). Hierarchical clustering was formed based on the proximity of relationship among attributes and treatments. Clusters obtained through heatmap were in conformity with the PCA clustering. Presence of days required for appearing first leaf and protein content were out grouped which was also observed in PCA depicted that these two attributes somehow are unique and showed different trends than the others.

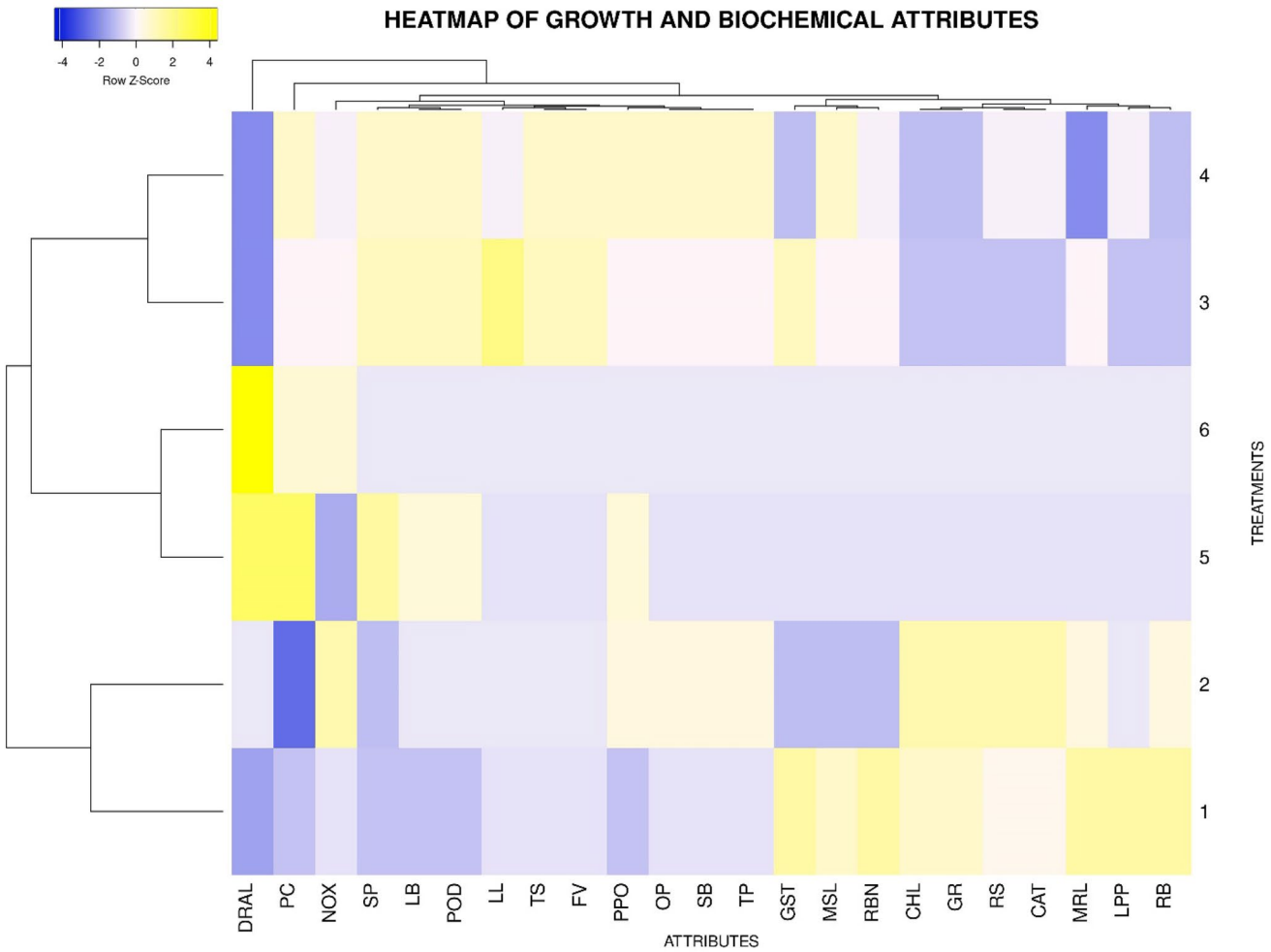

Fig. 7 Heat map analysis of different treatments and variables. 1 = FeNP 10, 2 = FeNP EDTA 10, 3 = FeNP 50, 4 = FeNP EDTA 50, 5 = FeSO4, 6 = Control. *DRAL* days required for appearing first leaf, *PC* protein content, *NOX* NADPH oxidase, *SP* sprouting percentage, *LB* leaf breadth, *POD* peroxidase, *LL* leaf length, *TS* total sugar, *FV* flavonol, *PPO* polyphenol oxidase, *OP* ortho dihydric phenol, *SB* shoot biomass, *TP* total phenol, *GST* glutathione s transferase, *MSL* minimum shoot length, *RBN* root branching number, *CHL* chlorophyll, *GR* glutathione reductase, *RS* reducing sugar, *CAT* catalase, *MRL* maximum root length, *LPP* number of leaves per plant, *RB* root biomass

Probable Mechanism of Action

The overall results obtained indicated strong potential of iron oxide nanoparticles and EDTA functionalized iron oxide nanoparticles to serve as a leading Fe-enriching micronutrients fertilizer for enhanced agricultural production. However, understanding the method of these nanoparticles uptake and accumulation in plant tissue is important for both practical applicability and safety. It is difficult to investigate interaction of nanoparticles with complex biological system like plants through a single experiment or via a single independent material characterization technique because of presence of low concentration of nanoparticles in the plant tissue and the similarity of nanoparticles with naturally occurring nanoparticles and metal ions (Boutchuen et al. 2019). Uptake of nanoparticles greatly depends upon nature of nanoparticles itself, its size, shape, chemical composition etc. (Rico et al. 2011). Judy et al. (2012) suggested that functionalization and surface modification of the nanoparticles can change and alter its absorption properties and accumulation by the plants. Because of reported favorability of cheated Fe fertilizer uptake and transportation in plants, we engineered our iron oxide nanoparticles by surface functionalization using EDTA to investigate the efficacy of chelated iron nanoparticles.

Plant follows two mechanism viz. reduction-based strategy and chelation-based strategy for uptake of iron. Reduction-based strategy involves in acidification of rhizosphere; thereby increases available Fe (III) in roots' surroundings. Prior to its uptake by the iron-regulated transporter 1 (IRT1), root surface-localized ferric reductase oxidase 2 (FRO2) reduced Fe(III) to Fe(II) (Robinson et al. 1999; DiDonato et al. 2004). IRT1 is an Fe(II) transporter located at epidermal cells that eventually facilitates iron uptake in plants (Thomine and Vert 2013). The problem is that IRT1 has a broad specificity which also uptakes other divalent cations (zinc, cadmium, manganese, cobalt) thereby competing with iron absorption (Meda et al. 2007; Pineau et al. 2012; Lešková et al. 2017). On the other side, in chelation-based strategy plants release some phyto-siderophores (PS) in the root surroundings which forms Fe-PS chelate. These chelators are using yellow stripe-like (YSL) family of transporter protein to transport iron across the root plasma membrane.

For absorption of iron oxide nanoparticles, plant responses by acidification of rhizosphere through activation of H^+-ATPase, and secretion of different organic acids and phenolics for chelation of iron, and reduction of Fe(III) to Fe(II) by ferric reductase. In response to iron deficiency, AHA (plasma membrane localized H^+-ATPase) is known to pump protons across the plasma membrane (Jeong and Connolly 2009). The gene FRO2, which encodes ferric chelate reductase had an over-expression in *Citrus maxima* by application of Fe_2O_3 nanoparticles. However, the expression level of AHA was not influenced by maghemite application (Hu et al. 2017).

Plants have well developed mechanism for uptake, transportation, storage and remobilization of Fe^{+2} ions (Roschzttardtz et al. 2009). Roschzttardtz et al. (2013) confirmed that, in the apoplast of central cylinder, plant roots mainly accumulate iron. But problem is that like Fe^{+2} ions, FeNPs are not present in soluble form. By compiling all the evidence observed, Yuan et al. (2018) concluded that applied FeNPs may somehow converted into bio-available form (for example, Fe^{+3}/Fe^{+2}) and afterward transported towards the vascular tissues. These findings are also supported by Keller et al. (2012), who by application of FeNPs observed substantial increase in Fe^{+3} and/or Fe^{+2} concentrations. The apoplastic location and movement of FeNPs was previously supported by various viewpoints that typically nanoparticles of larger size (more than 20 nm) can't penetrate through cell walls (Rico et al. 2013; Martínez-Fernández and Komárek, 2016). Figure 8 shows a diagrammatic representation of the root strategies and possible routes for iron uptake and translocation into aerial plant parts.

Once the iron nanoparticles penetrate into the plants, they can follow two different paths to move through tissues i.e. apoplast or symplast. Apoplastic transport involve movement of water and substances through the extracellular spaces, xylem vessels and cell walls of adjacent cells and takes place outside the plasma membrane (Sattelmacher 2001), whereas in symplastic movement transportation takes place through the specialized structure called plasmodesmata (Roberts and Oparka 2003). Radial movement of nanoparticles within plant tissues was mainly triggered by apoplastic pathway which assists nanomaterials to reach the root central cylinder and the vascular tissues (Larue et al. 2012; Zhao et al. 2012; Sun et al. 2014). Once it reaches the central cylinder, following the transpiration stream nanoparticles can further move upward to the aerial part through xylem (Cifuentes et al. 2010; Wang et al. 2012; Sun et al. 2014). However, through apoplastic pathway transportation can be stopped at casparian strip (Larue et al. 2012; Sun et al. 2014; Lv et al. 2015) and some nanomaterials can be accumulated there. To overcome this hydrophobic layer, they have to follow symplastic pathway via endodermal cells (Robards and Robb 1972). Symplastic transport is also possible in the phloem using sieve tube elements, which allow distribution towards non photosynthetic tissues and organs (Wang et al. 2012; Raliya et al. 2016).

On the other hand, in case of foliar applications, nanoparticles have to cross cuticular barrier following the lipophilic or hydrophilic pathway (Schönherr 2002). In lipophilic pathway diffusion takes place trough cuticular waxes, whereas the hydrophilic pathway involves dispersion through polar aqueous pores of cuticle or stomata (Eichert et al. 2008; Eichert and Goldbach, 2008). In comparison to cuticular

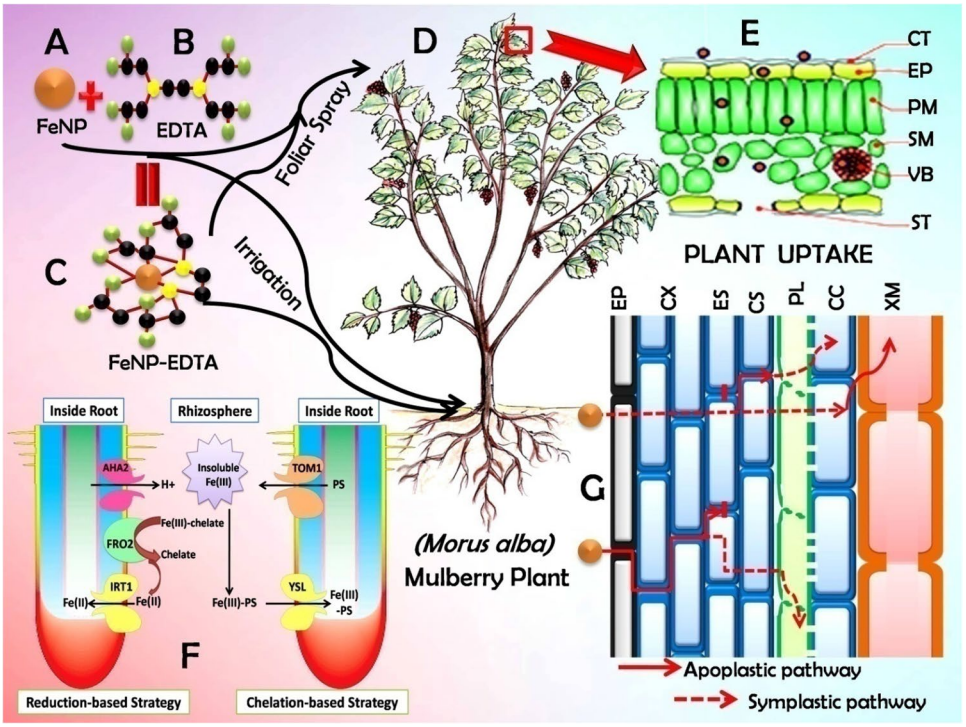

Fig. 8 Probable mechanism of iron nanoparticles uptake and translocation in plants, **A** iron oxide nanoparticles, **B** EDTA, **C** EDTA functionalized iron oxide nanoparticles, **D** mulberry plant, **E** foliar uptake, **F** root strategy to uptake iron, **G** translocation of uptaken nanoparticles through vascular system. *CT* cuticle, *EP* epidermis, *PM* palisade mesophyll, *SM* spongy mesophyll, *VB* vascular bundle, *ST* Stoma, *CX* cortex, *ES* epidermis, *CS* casparian strip, *PL* phloem, *CC* companion cell, *XM* xylem

pores (pore diameter-2 nm), the stomatal diffusion pathway appears as more appropriate route for nanomaterials penetration with a size exclusion limit of more than 10 nm (Eichert et al. 2008). Nanoparticles after entering the leaf apoplast through stomatal pathway may undergo long distance transport through vascular system. Previous reports suggested that sugars, photosynthate and other macromolecules reside in the leaf can be transported downward to the shoot and root through phloem (Lough and Lucas, 2006). Wang et al. (2013) by applying four metal oxide nanoparticles (size ranges 24–47 nm) in watermelon plant observed that small sized nanoparticles can penetrate the leaf and can reached the shoots and roots. The results indicated the ability of nanoparticles uptake by leaf to reach the roots through phloem sieve tubes.

Conclusion

In summary, this work reports the effects of iron oxide nanoparticles and EDTA functionalized iron oxide nanoparticles on the phenotypic characteristics of *Morus alba,* showing enhancement in biomass and different growth attributes. Applied nanoparticles also exhibited greater impact on several biochemical and antioxidant enzymes attributes. These nanoparticles might be an ideal substitution for the traditional iron fertilizer and will be helpful in fortification of plants with nutritional value. However, some points like the mechanism behind the transformation of FeNP into available form, mobilization, sequestration and accumulation of nanoparticles should be investigated and improvement in understanding the toxicological effects like generations of ROS through FeNPs oxidation will require further study.

Acknowledgements The author would like to thank Department of Science and Technology and Biotechnology, Government of West Bengal for financial assistance [Grant No- 263(Sanc.)/ST/P/S&T/1G-65/2017]. The author would also like to thank SAIF, IIT Bombay and STIC, Cochin University of Science and Technology for assisting while conducting different instrumental analysis.

Author Contribution First author (MSH) has conducted the overall experiment, collected samples, performed software analysis, analyzed the data and primarily drafted the manuscript. Second author (SG) assisted while performing the trial on mulberry, also helps in biochemical assay. Corresponding author (PM) conceptualized the work, help in reviewing and revising the manuscript and data.

Declarations

Conflict of interest The authors report no conflict of interest. The authors alone are responsible for the content and writing of the articles, also the work was purely conducted for research purpose only.

References

Alkhatib R, Alkhatib B, Abdo N, AL-Eitan L, Creamer R, (2019) Physio-biochemical and ultrastructural impact of (Fe_3O_4) nanoparticles on tobacco. BMC Plant Biol 19:253. https://doi.org/10.1186/s12870-019-1864-1

Allsopp A (1954) Juvenile stages of plants and the nutritional status of the shoot apex. Nature 173:1032–1035. https://doi.org/10.1038/1731032a0

Arnon DI (1949) Estimation of chlorophyll (DMSO). Plant Physiol 24:1–15

Askary M, Talebi SM, Amini F, Bangan ADB (2017) Effects of iron nanoparticles on *Mentha piperita* L. under salinity stress. Biologija 63(1):65–75

Asl KR, Hosseini B, Sharafi A, Palazon J (2019) Influence of nano-zinc oxide on tropane alkaloid production, *h6h* gene transcription and antioxidant enzyme activity in *Hyoscyamus reticulates* L. hairy roots. Eng Life Sci 19:73–89

Atanassova M, Georgieva S, Ivancheva K (2011) Total phenolic and total flavonoid contents, antioxidant capacity and biological contaminants in medicinal herbs. J Chem Technol Metall 46:81–88

Auffan M, Rose J, Bottero JY, Lowry GV, Jolivet JP, Wiesner MR (2009) Towards a definition of inorganic nanoparticles from an environmental, health and safety perspective. Nat Nanotechnol 4:634–641

Babicki S, Arndt D, Marcu A, Liang Y, Grant JR, Maciejewski A, David S, Wishart DS (2016) Heatmapper: web-enabled heat mapping for all. Nucleic Acids Res. https://doi.org/10.1093/nar/gkw419

Balk J, Lobréaux S (2005) Biogenesis of iron-sulfur proteins in plants. Trends Plant Sci 10:1360–1385. https://doi.org/10.1016/j.tplants.2005.05.002

Becana M, Moran JF, Iturbe-Ormaetxe I (1998) Iron-dependent oxygen free radical generation in plants subjected to environmental stress: toxicity and antioxidant protection. Plant Soil 201:137–147

Bhardwaj D, Ansari MW, Sahoo RK et al (2014) Biofertilizers function as key player in sustainable agriculture by improving soil fertility, plant tolerance and crop productivity. Microb Cell Fact 13:66. https://doi.org/10.1186/1475-2859-13-66

Bindraban PS, Dimkpa C, Nagarajan L, Roy A, Rabbinge R (2015) Revisiting fertilizers and fertilization strategies for improved nutrient uptake by plants. Biol Fertil Soils 51:897–911. https://doi.org/10.1007/s00374-015-1039-7

Boutchuen A, Zimmerman D, Aich N, Masud AM, Arabshahi A, Palchoudhury S (2019) Increased plant growth with hematite nanoparticle fertilizer drop and determining nanoparticle uptake in plants using multimodal approach. J Nanomater. https://doi.org/10.1155/2019/6890572

Briat JF, Curie C, Gaymard F (2007) Iron utilization and metabolism in plants. Curr Opin Plant Biol 10:276–282

Cifuentes Z, Custardoy L, de la Fuente JM, Marquina C, Ibarra MR, Rubiales D et al (2010) Absorption and translocation to the aerial part of magnetic carbon-coated nanoparticles through the root of different crop plants. J Nanobiotechnol 8:26. https://doi.org/10.1186/1477-3155-8-26

da Silva CR, Koblitz MGB (2010) Partial characterization and inactivation of peroxidases and polyphenol-oxidases of Umbu-Caja (Spondias spp). CiêncTecnol Aliment 30(3):790–796. https://doi.org/10.1590/S0101-20612010000300035

DiDonato RJ Jr, Roberts LA, Sanderson T, Eisley RB, Walker EL (2004) Arabidopsis Yellow Stripe-Like2 (YSL2): a metal-regulated gene encoding a plasma membrane transporter of nicotianamine-metal complexes. Plant J 39(3):403–414. https://doi.org/10.1111/j.1365-313X.2004.02128.x

Eichert T, Goldbach HE (2008) Equivalent pore radii of hydrophilic foliar uptake routes in stomatous and astomatous leaf surfaces further evidence for a stomatal pathway. Physiol Plant 132:491–502. https://doi.org/10.1111/j.1399-3054.2007.01023.x

Eichert T, Kurtz A, Steiner U, Goldbach HE (2008) Size exclusion limits and lateral heterogeneity of the stomatal foliar uptake pathway for aqueous solutes and water-suspended nanoparticles. Physiol Plant 134:151–160. https://doi.org/10.1111/j.1399-3054.2008.01135.x

Elanchezhiana R, Kumarb D, Ramesha K, Biswasa AK, Guheyb A, Patraa AK (2017) Morpho-physiological and biochemical response of maize (Zea mays L. plants fertilized with nano-iron (Fe3O4) micronutrient. J Plant Nutr 40(14):1969–1977. https://doi.org/10.1080/01904167.2016.1270320

Elemike EE, Uzoh IM, Onwudiwe DC, Babalola OO (2019) The role of nanotechnology in the fortification of plant nutrients and improvement of crop production. Appl Sci 9:499. https://doi.org/10.3390/app9030499

El-Temsah YS, Oughton DH, Joner EJ (2014) Effectsofnano-sized zero-valent ironon DDT degradation and residual toxicity in soil: a column experiment. Plant Soil 368:189–200. https://doi.org/10.1016/j.chemosphere.2013.02.039

Ende WV (2014) Sugars take a central position in plant growth, development and stress responses. A focus on apical dominance. Front Plant Sci. https://doi.org/10.3389/fpls.2014.00313

Eslami S, Ebrahimzadeh MA, Biparva P (2018) Green synthesis of safe zero valent iron nanoparticles by *Myrtus communis* leaf extract as an effective agent for reducing excessive iron in iron-overloaded mice, a thalassemia model. RSC Adv 8:26144–26155. https://doi.org/10.1039/C8RA04451A

Fernández V, Eichert T, Del Río V, López-Casado G, Heredia-Guerrero JA, Abadía A, Heredia A, Abadía J (2008) Leaf structural changes associated with iron deficiency chlorosis in field-grown pear and peach: physiological implications. Plant Soil. https://doi.org/10.1007/s11104-008-9667-4

Geetha T, Ramamoorthy R, Murugan N (2017) Effect of Foliar Spray of Micronutrients Applied Individually and in Combination on Mulberry Leaf Production, Cocoon Productivity and Profitability S. Vignesh, A. Philip Arokiadoss (ed.), Statistical Approaches on Multidisciplinary Research, Volume I, Surragh Publishers, India

Ghafari H, Razmjoo J (2013) Effect of foliar application of nano-iron oxidase, iron chelate and iron sulphate rates on yield and quality of wheat. Int J Plant Prod 4(11):2997–3003

Ghafariyan MH, Malakouti MJ, Dadpour MR, Stroeve P, Mahmoudi M (2013) Effects of magnetite nanoparticles on soybean chlorophyll. Environ Sci Techcnol 47:10645–10652

Ghasemzadeh A, Nasiri A, Jaafar HZE, Baghdadi A, Ahmed I (2014) Changes in phytochemical synthesis, chalcone synthase activity and pharmaceutical qualities of sabah snake grass in relation to plant age. Molecules. https://doi.org/10.3390/molecules191117632

Ghrair AM, Ingwersen J, Streck T (2010) Immobilization of heavy metals in soils amended by nanoparticulate zeolitic tuff: sorption-desorption of cadmium. J Plant Nutr Soil Sci 173:852–860. https://doi.org/10.1002/jpln.200900053

Hänsch R, Mendel RR (2009) Physiological functions of mineral micronutrients (Cu, Zn, Mn, Fe, Ni, Mo, B, Cl). Curr Opin Plant Biol 12(3):259–266. https://doi.org/10.1016/j.pbi.2009.05.006

Hartmann HT, Kester DE, Devies FT, Geneve RL (2002) Plant Propagation: Principles and Practices, 7th edn. Prentice-Hall, Englewood Cliffs, N.J.

Hartmann HT, Kester DE, Davies FT, Geneve RL (2011) Hartmann and Kester's plant propagation-principles and practices. Prentice Hall, New Jersey

Hasanuzzaman M, Hossain MA, Fujita M (2011) Nitric oxide modulates antioxidant defense and the methylglyoxal detoxification system and reduces salinity-induced damage of wheat seedlings. Plant Biotechnol Rep 5:353–365. https://doi.org/10.1007/s11816-011-0189-9

Hilo A, Shahinnia F, Druege U, Franken P, Melzer M, Rutten T, Wirén NV, Hajirezaei MR (2017) A specific role of iron in promoting meristematic cell division during adventitious root formation. J Exp Bot. https://doi.org/10.1093/jxb/erx248

Hu J, Guo H, Li J, Gan Q, Wang Y, Xing B (2017) Comparative impacts of iron oxide nanoparticles and ferric ions on the growth of *Citrus maxima*. Environ Pollut 221:199–208. https://doi.org/10.1016/j.envpol.2016.11.064

Jeong J, Connolly EL (2009) Iron uptake mechanisms in plants: functions of the FRO family of ferric reductases. Plant Sci 176(6):709–714

Ju M, Navarreto-Lugo M, Wickramasinghe S, Milbrandt NB, McWhorter A, Samia ACS (2019) Exploring the chelation-based plant strategy for iron oxide nanoparticle uptake in garden cress (*Lepidium sativum*) using magnetic particle Spectrometry. Nanoscale 11:18582–18594. https://doi.org/10.1039/C9NR05477D

Judy JD, Unrine JM, Rao W, Wirick S, Bertsch PM (2012) Bioavailability of gold nanomaterials to plants: importance of particle size and surface coating. Environ Sci Technol 46:8467–8474. https://doi.org/10.1021/es3019397

Kadam VB, Momin RK, Fatima S, Kadam UB (2013) Estimation of total phenol in different plant parts of genus *Sesbania* in Maharastra. Intl J Pharma and Bio Sci 2(4):202–206

Keller AA, Garner K, Miller RJ, Lenihan HS (2012) Toxicity of nano-zero valent iron to fresh water and marine organisms. Plos One 7:e43983

Khan MB, Rafiq R, Hussain M, Farooq M, Jabran K (2012) Ridge sowing improves root system, phosphorus uptake, growth and yield of maize (*Zea mays* L.) hybrids. J Anim Plant Sci 22:309–317

Khan A, Najeeb U, Wang L, Tan DKY, Yang G, Munsif F (2017) Planting density and sowing date strongly influence growth and lint yield of cotton crops. Field Crops Res. https://doi.org/10.1016/j.fcr.2017.04.019

Kim J, Rees DC (1992) Structural models for the metal centers in the nitrogenous molybdenum-iron protein. Science 257:1677–1682

Kim JH, Kim D, Seo SM, Kim D (2019) Physiological effects of zero-valent iron nanoparticles in rhizosphere on edible crop, *Medicago sativa* (Alfalfa), grown in soil. Ecotoxicol 28:869–877

Kirschbaum MUF (2011) Does enhanced photosynthesis enhance growth? Lessons learned from CO_2 enrichment studies. Plant Physiol 155:117–124. https://doi.org/10.1104/pp.110.166819

Kobayashi T, Nishizawa NK (2012) Iron uptake, translocation and regulation in higher plants. Annu Rev Plant Biol 63:131–152. https://doi.org/10.1146/annurev-arplant-042811-105522

Kraus EJ, Kraybill HR (1918) Vegetation and Reproduction with Special Reference to the Tomato. Station bulletin (Oregon Agricultural Experiment Station). Corvallis, OR: Oregon Agricultural College Experiment Station**.**

Larue C, Veronesi G, Flank AM, Surble S, Herlin-Boime N, Carrière M (2012) Comparative uptake and impact of TiO2 nanoparticles in wheat and rapeseed. J Toxicol Environ Health A 75:722–734. https://doi.org/10.1080/15287394.2012.689800

Laware SL, Raskar S (2014) Effect of titanium dioxide nanoparticles on hydrolytic and antioxidant enzymes during seed germination in onion. Int J Curr Microbiol Appl Sci 3(7):749–760

Lešková A, Giehl RFH, Hartmann A, Fargašová A, von Wirén N (2017) Heavy Metals Induce Iron Deficiency Responses at Different Hierarchic and Regulatory Levels. Plant Physiol 174(3):1648–1668. https://doi.org/10.1104/pp.16.01916

Li W, Lan P (2017) The understanding of the plant iron deficiency responses in strategy i plants and the role of ethylene in this process by omic approaches. Front Plant Sci. https://doi.org/10.3389/fpls.2017.00040

Loeb J (1924). Regeneration from a Physic-Chemical Viewpoint. New York, NY: McGRaw-Hill.

López-Millán AF, Duy D, Philippar K (2016) Chloroplast iron transport proteins – function and impact on plant physiology. Front Plant Sci 7:178. https://doi.org/10.3389/fpls.2016.00178

Lopez-Vargas ER, Ortega-ortiz H, Cadenas-pliego G, De-Alba-Romenus K, Cabrera-De-La-Fuente M, Benavides-Mendoza A, Juarez-Maldonado A (2018) Foliar application of copper nanoparticles increases the fruit quality and the content of bioactive compounds in tomatoes. Appl Sci 8(7):1020. https://doi.org/10.3390/app8071020

Lough TJ, Lucas WJ (2006) Integrative plant biology: role of phloem long-distance macromolecular trafficking. Annu Rev Plant Biol 57:203–232

Lowry OH, Rosebrough NJ, Farr AL, Randall RJ (1951) Protein measurement with the folin phenol reagent. J Biol Chem 193(1):265–275

Lu JW, Chen F, Yu CB (2003) Study on the soil nutrition status of mulberry gardens in Hubei. I. Classification of soil nutrient content for mulberry fields in Hubei. Hubei Agricult Sci 2:50–53

Lv J, Zhang S, Luo L, Zhang J, YangcK CP (2015) Accumulation, speciation and uptake pathway of ZnO nanoparticles in maize. Environ Sci Nano 2:68–77. https://doi.org/10.1039/c4en00064a

Magdalena AG, Silva IMB, Marques RFC, Pipi ARF, Lisboa-Filho PN, Jafelicci M Jr (2018) EDTA-functionalized Fe_3O_4 nanoparticles. J Phys Chem Solids 113:5–10. https://doi.org/10.1016/j.jpcs.2017.10.002

Mahadevan A, Sridhar R (1986) Methods in physiological plant pathology. Sivakami Publication, Chennai

Mahmoud AWM, Abdelaziz SM, El-Mogy MM, Abdeldaym EA (2019) Effect of foliar ZnO and FeO nanoparticles application on growth and nutritional quality of red radish and assessment of their accumulation on human health. Agriculture (poľnohospodárstvo) 65(1):16–29. https://doi.org/10.2478/agri-2019-0002

Majeed A, Minhas WA, Mehboob N, Farooq S, Hussain M, Alam S et al (2020) Iron application improves yield, economic returns and grain-Fe concentration of mungbean. PLoS One. https://doi.org/10.1371/journal.pone.0230720

Manzano AI, Larkin OJ, Dijkstra CE, Anthony P, Davey MR, Eaves L, Hill RJ, Herranz R, Medina FJ (2013) Meristematic cell proliferation and ribosome biogenesis are decoupled in diamagnetically levitated Arabidopsis seedlings. BMC Plant Biol 13:124

Martínez-Fernández D, Komárek M (2016) Comparative effects of nanoscale zero-valent iron (nZVI) and Fe_2O_3 nanoparticles on root hydraulic conductivity of *Solanum lycopersicum* L. Environ Exp Bot 131:128–136

Meda AR, Scheuermann EB, Prechsl UE, Erenoglu B, Schaaf G, Hayen H, Weber G, von Wirén N (2007) Iron acquisition by phytosiderophores contributes to cadmium tolerance. Plant Physiol 143(4):1761–1773. https://doi.org/10.1104/pp.106.094474

Metsalu T, Vilo J (2015) Clustvis: a web tool for visualizing clustering of multivariate data using Principal Component Analysis and heatmap. Nucleic Acids Res. https://doi.org/10.1093/nar/gkv468

Mimmo T, DelBuono D, Terzano R, Tomasi N, Vigani G, Crecchio R et al (2014) Rhizospheric organic compounds in the soil–microorganism– plant system: the irrolein iron availability. Eur J Soil Sci 65:629–642. https://doi.org/10.1111/ejss.12158

Mittler R (2002) Oxidative stress, antioxidants and stress tolerance. Trends Plant Sci 7:405–410

Moore B, Zhou L, Rolland F, Hall Q, Cheng WH, Liu YX et al (2003) Role of the Arabidopsis glucose sensor HXK1 in nutrient, light, and hormonal signalling. Science. https://doi.org/10.1126/science.1080585

Noor-Ul-Din S (2012) Seasonal variation in nutrient components of mulberry leaf and their uptake in response to split applications of NPK under temperate conditions. Ph.D thesis submitted to Sher-e-Kashmir University of Agricultural Sciences & Technology of Kashmir, pp: 121–122. http://krishikosh.egranth.ac.in/handle/1/5810003620

Palchoudhury S, Jungjohann KL, Weerasena L et al (2018) Enhanced legume root growth with pre-soaking in α-Fe_2O_3 nanoparticle

fertilizer. RSC Adv 8:24075–24083. https://doi.org/10.1039/C8RA04680H
Pan G, Lou CF (2008) Isolation of an 1-aminocyclopropane-1-carboxylate oxidase gene from mulberry (*Morus alba* L.) and analysis of the function of this gene in plant development and stresses response. J Plant Physiol 165:1204–1213
Panda D, Sarkar RK (2012) Leaf photosynthetic activity and antioxidant defense associated with Sub1 QTL in rice subjected to submergence and subsequent re-aeration. Rice Sci. https://doi.org/10.1016/S1672-6308(12)60029-8
Pineau C, Loubet S, Lefoulon C, Chalies C, Fizames C, Lacombe B, Ferrand M, Loudet O, Berthomieu P, Richard O (2012) Natural variation at the *FRD3* MATE transporter locus reveals cross-talk between Fe Homeostasis and Zn tolerance in *Arabidopsis thaliana*. Plos Genet 8:e1003120. https://doi.org/10.1371/journal.pgen.1003120
Poorter H, Nagel O (2000) The role of biomass allocation in the growth response of plants to different levels of light, CO_2, nutrients and water: a quantitative review. Aust J Plant Physiol 27:595–607
Prasad A, Sedlářová M, Balukova A, Rác M, Pospíšil P (2020) Reactive oxygen species as a response to wounding: In Vivo Imaging in *Arabidopsis thaliana*. Front Plant Sci. https://doi.org/10.3389/fpls.2019.01660
Raines CA (2011) Increasing photosynthetic carbon assimilation in C_3 plant to improve crop yield: current and future strategies. Plant Physiol. https://doi.org/10.1104/pp.110.168559
Raliya R, Franke C, Chavalmane S, Nair R, Reed N, Biswas P (2016) Quantitative understanding of nanoparticle uptake in watermelon plants. Front Plant Sci 7:1288. https://doi.org/10.3389/fpls.2016.01288
Rani P, Meena Unni K, Karthikeyan J (2004) Evaluation of antioxidant properties of berries. Indian J Clin Biochem 19:103–110. https://doi.org/10.1007/BF02894266
Rastogi A, Zivcak M, Sytar O, Kalaji HM, He X, Mbarki S, Brestic M (2017) Impact of metal and metal oxide nanoparticles on plant: a critical review. Front Chem. https://doi.org/10.3389/fchem.2017.00078
Raya KB, Ahmad SH, Farhana SF, Mohammad M, Tajidin NE, Parvez A (2015) Changes in phytochemical contents in different parts of *Clinacanthus nutans* (Burm. f.) lindau due to storage duration. Bragantia, Campinas 74:445–452. https://doi.org/10.1590/1678-4499.0469
Rico CM, Majumdar S, Duarte-Gardea M, Peralta-Videa JR, Gardea-Torresdey JL (2011) Interaction of nanoparticles with edible plants and their possible implications in the food chain. J Agric Food Chem 59:3485–3498. https://doi.org/10.1021/jf104517j
Rico CM, Morales MI, Barrios AC et al (2013) Effect of cerium oxide nanoparticles on the quality of rice (Oryza sativa L.) grains. J Agric Food Chem 61(47):11278–11285. https://doi.org/10.1021/jf404046v
Robards AW, Robb ME (1972) Uptake and binding of uranyl ions by barley roots. Science 178:980–982. https://doi.org/10.1126/science.178.4064.980
Roberts AG, Oparka KJ (2003) Plasmodesmata and the control of symplastic transport. Plant Cell Environ 26:103–124. https://doi.org/10.1046/j.1365-3040.2003.00950.x
Robinson NJ, Procter CM, Connolly EL, Guerinot ML (1999) A ferric-chelate reductase for iron uptake from soils. Nature 397:694–697. https://doi.org/10.1038/17800
Roschzttardtz H, Conéjéro G, Curie C, Mari S (2009) Identification of the endodermal vacuole as the iron storage compartment in the *Arabidopsis* embryo. Plant Physiol 151:1329–1338
Roschzttardtz H, Grillet L, Isaure MP, Conéjéro G, Ortega R, Curie C, Mari S (2011) Plant cell nucleolus as a hot spot for iron. J Biol Chem 286:27863–27866
Roschzttardtz H, Conéjéro G, Divol G et al (2013) New insights into Fe localization in plant tissues. Front Plant Sci. https://doi.org/10.3389/fpls.2013.00350
Rout GR, Sahoo S (2015) Role of iron in plant growth and metabolism. Rev Agric Sci 3:1–24. https://doi.org/10.7831/ras.3.1
Rowe DB, Blazich FA, Weir RJ, Carolina N (1999) Mineral nutrient and carbohydrate status of loblolly pine during mist propagation as influenced by stock plant nitrogen fertility. HortScience 34:1279–1285
Rui M, Ma C, Hao Y, Guo J, Rui Y, Tang X, Zhao Q, Fan X, Zhang Z, Hou T, Zhu S (2016) Iron Oxide Nanoparticles as a Potential Iron Fertilizer for Peanut (*Arachis hypogaea*). Front Plant Sci 7:815. https://doi.org/10.3389/fpls.2016.00815
Sadasivam S, Manickam A (1996) Biochemical Methods (Second Ed.). New Age International (P) Ltd. and Tamil Nadu Agricultural University, Coimbatore
Samaranayake P, Peiris BD, Dssanayake S (2012) Effect of excessive ferrous (Fe 2+) on growth and iron content in rice (*Oryza sativa*). Int J Agr Biol 14:296–298
Sattelmacher B (2001) The apoplast and its significance for plant mineral nutrition. New Phytol 149:167–192. https://doi.org/10.1046/j.1469-8137.2001.00034.x
Savatin DV, Gramegna G, Modesti V, Cervone F (2014) Wounding in the plant tissue: the defense of a dangerous passage. Front Plant Sci. https://doi.org/10.3389/fpls.2014.00470
Schönherr J (2002) A mechanistic analysis of penetration of glyphosate salts across astomatous cuticular membranes. Pest Manag Sci 58:343–351. https://doi.org/10.1002/ps.462
Senge MO, Ryan AA, Letchford KA, MacGowan SA, Mielke T (2014) Chlorophylls, Symmetry, Chirality, and Photosynthesis. Symmetry 6(3):781–843. https://doi.org/10.3390/sym6030781
Sheykhbaglou R, Sedghi M, Shishevan MT, Sharifi RS (2010) Effects of nano-iron oxide particles on agronomic traits of soybean. Not Sci Biol 2(2): 112–113. https://doi.org/10.15835/nsb224667
Shigeoka S, Ishikawa T, Tamoi M, Miyagawa Y, Takeda T, Yabuta Y, Yoshimura K (2002) Regulation and function of ascorbate peroxidase isoenzymes. J Exp Bot 53:1305–1319
Straub KL, Benz M, Schink B (2001) Iron metabolism in anoxic environments at near neutral pH. FEMS Microbiol Ecol 34(3):181–186. https://doi.org/10.1111/j.1574-6941.2001.tb00768.x
Sun D, Hussain HI, Yi Z, Siegele R, Cresswell T, Kong L et al (2014) Uptake and cellular distribution, in four plant species, of fluorescently labeled mesoporous silica nanoparticles. Plant Cell Rep 33:1389–1402. https://doi.org/10.1007/s00299-014-1624-5
Svenson SE, Davies FT (1995) Change in tissue mineral elemental concentration during root initiation and development of poinsettia cuttings. HortScience 30:617–619
Tagliavini M, Abadía J, Rombolà AD, Abadía A, Tsipouridis C, Marangoni B (2000) Agronomic means for the control of iron deficiency chlorosis in deciduous fruit trees. J Plant Nutr. https://doi.org/10.1080/01904160009382161
Taranto F, Pasqualone A, Mangini G et al (2017) Polyphenol Oxidases in Crops: Biochemical, Physiological and Genetic Aspects. Int J Mol Sci 18(2):377. https://doi.org/10.3390/ijms18020377
Thimmaiah SR (2004) Standard methods of biochemical analysis. Kalyani publishers, New Delhi, India
Thomine S, Vert G (2013) Iron transport in plants: better be safe than sorry. CurrOpin Plant Biol 16(3):322–327. https://doi.org/10.1016/j.pbi.2013.01.003
Vadivel N, Rajendran V, Suriyaprabha R, Yuvakkumar R (2012) Catalytic effect of iron nanoparticles on heterocyst, protein and chlorophyll content of catalytic effect of iron nanoparticles on heterocyst. Int J Green Nanotechnol 4:326–338
Wang Z, Xie X, Zhao J, Liu X, Feng W, White JC et al (2012) Xylem- and phloem-based transport of CuO nanoparticles in maize (*Zea*

mays L.). Environ Sci Technol 46:4434–4441. https://doi.org/10.1021/es204212z

Wang WN, Tarafdar JC, Biswas P (2013) Nanoparticle synthesis and delivery by an aerosol route for watermelon plant foliar uptake. J Nanopart Res 15:1417. https://doi.org/10.1007/s11051-013-1417-8

Wang Y, Jing H, Zhaoyi D, Junli L, Jin H (2016) In vitro assessment of physiological changes of watermelon (*Citrullus lanatus*) upon iron oxide nanoparticles exposure. Plant Physiol Biochem 108:353–360

Wilson PJ, John GKT (1999) Hodgson specific leaf area and leaf dry matter content as alternative predictors of plant strategies. New Phytol 143:155–162

Yang X, Yang L, Zheng H (2010) Hypolipidemic and antioxidant effects of mulberry (Morus alba L.) fruit in hyperlipidaemia rats. J Food ChemToxicol 48:2374–2379

Ye L, Li L, Wang L, Wang S, Li S, Du J et al (2015) MPK3/MPK6 are involved in iron deficiency-induced ethylene production in *Arabidopsis*. Front Plant Sci 6:953. https://doi.org/10.3389/fpls.2015.00953

Yoon H, Kang YG, Chang YS, Kim JH (2019) Effects of Zerovalent Iron Nanoparticles on Photosynthesis and Biochemical Adaptation of Soil-Grown *Arabidopsis thaliana*. Nanomater 9(11):1543. https://doi.org/10.3390/nano9111543

Yuan J, Chen Y, Li H et al (2018) New insights into the cellular responses to iron nanoparticles in *Capsicum annuum*. Sci Rep 8(1):3228. https://doi.org/10.1038/s41598-017-18055-w

Zayed BA, Salem AKM, Sharkawy HME (2011) Effect of different micronutrient treatments on rice (*Oriza sativa* L.) growth and yield under saline soil conditions. World J Agric Sci 7:179–184

Zhang HZ, Khan A, Tan DKY, Luo HH (2017) Rational water and nitrogen management improves root growth, increases yield and maintains water use efficiency of cotton under mulch drip irrigation. Front Plant Sci. https://doi.org/10.3389/fpls.2017.00912

Zhang Y, Li Y, He Y, Hu W et al (2018) Identification of NADPH oxidase family members associated with cold stress in strawberry. FEBS Open Bio 8:593–605. https://doi.org/10.1002/2211-5463.12393

Zhao L, Peralta-Videa JR, Ren M, Varela-Ramirez A, Li C, Hernandez-Viezcas JA et al (2012) Transport of Zn in a sandy loam soil treated with ZnO NPs and uptake by corn plants: electron microprobe and confocal microscopy studies. Chem Eng J 184:1–8. https://doi.org/10.1016/j.cej.2012.01.041

Zuo Y, Zhang F (2011) Soil and crop management strategies to prevent iron deficiency in crops. Plant Soil. https://doi.org/10.1007/s11104-010-0566-0